

# Measuring state-of-order by dielectric response: A comprehensive review on Fröhlich entropy estimation<sup>☆</sup>

Jacopo Parravicini<sup>a,b,\*</sup>, Gianbattista Parravicini<sup>c,1</sup>

<sup>a</sup> Dipartimento di Fisica & Astronomia, Università di Firenze, IT-50019 Sesto Fiorentino, Italy

<sup>b</sup> LENS - European Laboratory for Nonlinear Spectroscopy, IT-50019 Sesto Fiorentino, Italy

<sup>c</sup> Dipartimento di Fisica, Università di Pavia, IT-27100 Pavia, Italy

## ARTICLE INFO

### Keywords:

Dielectrics  
Entropy  
Experimental technique  
Dielectric spectroscopy  
Phase transitions  
Disorder

## ABSTRACT

The so-called *Fröhlich entropy* is the entropy variation of a material under the application of an electric field. This quantity can be calculated, under suitable hypotheses, from the measured real part of the static dielectric function, when the imaginary part is negligible. Although Fröhlich entropy is defined for a biased sample, a straightforward physical interpretation correlates it to the state-of-order of the considered physical system in absence of field. When Fröhlich entropy is calculated from experimental results, its trend is able to give several information about the evolution in temperature of the explored compound, especially of its phase transition features. We here provide a comprehensive review of the physical systems (dipolar liquids and nematics, organic molecular crystals, metallic nanoparticles, inorganic disordered ferroelectrics, etc.) where this approach has been exploited with the aim of evaluating their state of order and its temperature evolution. The variety of compounds where this method has been applied demonstrates that the estimation of the *Fröhlich entropy* can be considered a trustworthy tool for carrying out study on the state-of-order of different classes of materials. Indeed Fröhlich entropy evaluation can be considered a fruitful and reliable investigation technique which can be exploited alongside more usual experimental approaches.

## Introduction and landscape

The investigation of order/disorder degree of a given physical system has addressed by exploiting several experimental methods. The choice of which method should be employed depends on different features, such as what kind of system is considered, which sensitivity is requested, which temporal and/or temperature range should be detected, what complexity and which cost of the used instruments can be faced, etc. The exploited techniques are quite complicated, being employed to investigate both mesoscopic and microscopic realms. Strong attention is devoted to phase transitions in crystalline systems, where several concepts are involved, such as structural symmetries, stability, critical temperatures and amplitudes of phenomena, anisotropies, etc. Morphology and ordering are usually studied by the well known techniques employed in crystallography, such as X-ray diffractometry [1–3], X-ray absorption spectroscopy [4], EXAFS [5,6], electronic diffraction [7,8], neutron diffractometry [9,10], nuclear magnetic

resonance [3,11,12]. These techniques, when they are resolved in temperature, provide a description of the arrangement of sample internal symmetry, and the relative evolution when macroscopic thermodynamic parameters are changed. In fact, they are mainly based on the investigation in reciprocal space, so providing essential information on periodicity, where the presence of a specific kind of crystalline (or not) structure should be inspected. Instead, calorimetric techniques are based on different paradigms, which investigate the macroscopic energy states [13,14].

Among experimental techniques, on the other hand, dielectric spectroscopy is typically widely employed to characterize a given material [15–17]. When the dielectric properties are investigated as a function of temperature, such a technique is able to provide detailed information on the phases of the material. In this vein, an important use of dielectric spectroscopy employs a bias field spanning several frequencies. The measured dielectric response, thanks to the fluctuation–dissipation theorem, gives information on the molecular

<sup>☆</sup> This paper is dedicated to M. Bartozzi and V. Sanvito for their constant support.

\* Corresponding author at: Dipartimento di Fisica & Astronomia, Università di Firenze, IT-50019 Sesto Fiorentino, Italy.

E-mail address: [jacopo.parravicini@unifi.it](mailto:jacopo.parravicini@unifi.it) (J. Parravicini).

<sup>1</sup> Jacopo Parravicini and Gianbattista Parravicini equally contributed to all steps of the work.

arrangement of polarization fluctuations and on the dynamics of relaxation times [18,19]. Therefore, this approach must consider both real and imaginary part of the dielectric function and reconstruct a state of the matter by assuming specific models correlated to the time domain [20,21].

Conversely, the dielectric technique usually is not considered a method to *directly* explore the ordering of a system, similarly to what is done by calorimetric techniques, notably not time-dependent. Namely, an ideal pathway to obtain order information from dielectric physical quantities would be finding a correlation between them and thermodynamic quantities. The issue of bridging dielectrics and thermodynamics was considered for the first time in the theory of electrocaloric effect [22,23]; moreover, pyroelectric and piezocaloric effects are also described by equations involving thermodynamic variables [16,17,24–28]. In particular, finding the exact mathematical relationships among thermodynamic variables, electric and magnetic fields, susceptibility and dielectric displacement and magnetization fields, stresses and strains, made possible to extend Maxwell thermodynamic relations for anisotropic compounds [25,26,29–32]. However, the first comprehensive thermodynamic theory of a generic dielectrics was developed within a theoretical “rigorous treatment” [33]<sup>2</sup> by H. Fröhlich in Forties [34,35]. The following treatises, whose the main ones are by R. Becker [36], L. Landau [30], V. Daniel [37], C. Böttcher [38], and B.K.P. Scaife [39,40] employ the same concepts and obtain the same relationships. Specifically, Fröhlich considered an ideal dielectric undergone to an electric field. He was able to provide equations correlating the induced internal total energy, entropy, Helmholtz free energy with the dielectric quantities of the given material; they are called, respectively, *Fröhlich total energy*, *Fröhlich entropy* (FE), and *Fröhlich free energy* [41–43]. The most important result of these, however, is the estimation of the entropy induced by the application of a static electric field. Actually the found equation indicates that, under specific conditions, the induced entropy variation is proportional to the derivative of the *real part*  $\epsilon_s$  of the dielectric function with respect to the temperature  $T$ . Deep physical meaning of FE goes far beyond the thermodynamic description of a system in an *under-an-electric-field* condition. We quote Fröhlich himself from [35].<sup>3</sup>

“Finally, equation 3.12 [ $S = S_0(T) + (\partial\epsilon_s/\partial T)(E^2/8\pi)$ , i.e. Eq. (17) below] shows that the entropy is increased by the field if  $\partial\epsilon_s/\partial T$  is positive, and decreased if this quantity is negative. Since the entropy is a measure of the molecular disorder, an external field creates order in dipolar liquids and gases for which  $\epsilon_s$  decreases with increasing  $T$ . This may be expected because the field will orientate some of the dipoles which in the absence of a field are at random. In some dipolar solids, on the other hand  $\epsilon_s$  increases with  $T$ , which means that an external field increases the disorder. *This too is understandable if one assumes that in the absence of a field the dipoles are in a well-ordered state as may be expected in solids.* The field by turning some of the dipoles into different directions can thus only decrease the existing order”.<sup>4</sup>

Immediately after these sentences, in the same textbook the picture reported in Fig. 1 is inserted with the following caption:

“Schematic temperature-dependence of the dielectric constant  $\epsilon_s$  and of the entropy change  $S \propto \partial\epsilon_s/\partial T$  due to the polarization by a field. If  $S > 0$  the field creates disorder, if  $S < 0$  it creates order. Near the absolute zero of temperature the substance is *already* perfectly ordered. Hence  $\partial\epsilon_s/\partial T$  cannot be negative near  $T = 0$ ”.<sup>5</sup>

So Fröhlich states that, by analyzing the trend of the field-induced entropy (*Fröhlich entropy*), we can reconstruct the arrangement of the system “in the absence of field”. This fine argument of Fröhlich is the foundation of the here discussed experimental approach. On one hand the pure numerical single value of FE is only able to provide the thermodynamic quantity when the electric field is on; on the other hand, the analysis of its behavior as a function of the temperature is able to give deep information about the state of the system also in absence of an applied field. Exploiting FE evaluation to study the state-of-order of a system lays on this clever Fröhlich’s interpretation.

The recalled statements indicate that information about the state-of-order of a given system could be extracted, in principle, from its dielectric response. This gives the possibility of obtaining some thermodynamic information by exploiting dielectric techniques. Moreover, it enables to investigate the state-of-order through an approach which is usually not considered for such a kind of investigation and which is generally simpler and cheaper with respect to those above-mentioned.

Despite the significance of this thermodynamic approach was recognized by founders of the physics of dielectrics [30,36,37,40], no experimental studies involving his theory have been accomplished for more than forty years after Fröhlich’s publications. The first experimental use of Fröhlich equations and interpretation were carried out in 2003 by GianBattista Parravicini et al. for the investigation of melting processes in confined metallic nanoparticles [44–46]. Subsequently, Fröhlich arguments were fruitfully applied on the study of nematic compounds [47–51], molecular crystals [52,53], ferroelectric and glassy perovskites [41,43,54–57], polar glasses [58], polar and glass-forming liquids [33,59–62], polymeric films [63], enzymes [64]. The use of Fröhlich’s reasoning in describing so different systems demonstrates that it can be the basis of a powerful and trustworthy technique which, through the description of the order state, may give specific information on the temperature evolution of mesoscopic and microscopic physical systems. This provides results which are congruent and complementary with those obtained by the above-mentioned best-known methods.

In this review we intend to provide up-to-date landscape of the use of Fröhlich entropy in experimental studies. We analyze the required theoretical and experimental conditions where it can be used and how it has been exploited for describing several different physical systems, especially about phase transitions. The obtained wide outlook will demonstrate that Fröhlich entropy measurements can be accepted in the set of the trustworthy and well-consolidated methods, a further option which can be chosen, in alternative with respect to the standard investigation ways. This approach could be called *Fröhlich entropy evaluation* or *Fröhlich entropy technique*.

## Theory of Fröhlich entropy

The study of entropy in condensed matter pointed out that different entropic contributions can be inspected in materials. The discussion of these is faced in many works (e.g. [33,58,59,61,65–70]) which involve many subtle features. Instead, we here stress that Fröhlich’s arguments are solely based on standard principles of thermodynamics and basic electric field relationships. This simplicity assures the general validity of Fröhlich relationships and interpretations, which can be assumed as starting point for more detailed topics.<sup>6</sup>

<sup>2</sup> Pg. 6, note 7, of Ref. [33].

<sup>3</sup> Chapter 1, pages. 12–13.

<sup>4</sup> Emphasis added.

<sup>5</sup> Emphasis added.

<sup>6</sup> It is worth quoting G.P. Johari that, in 2016, wrote “In his rigorous treatment of thermodynamic effects of an electric field, Fröhlich derived Eq. (1) [the same of our Eq. (20)] for the entropy change by making two assumptions”, from [33], pg. 6, note 7.

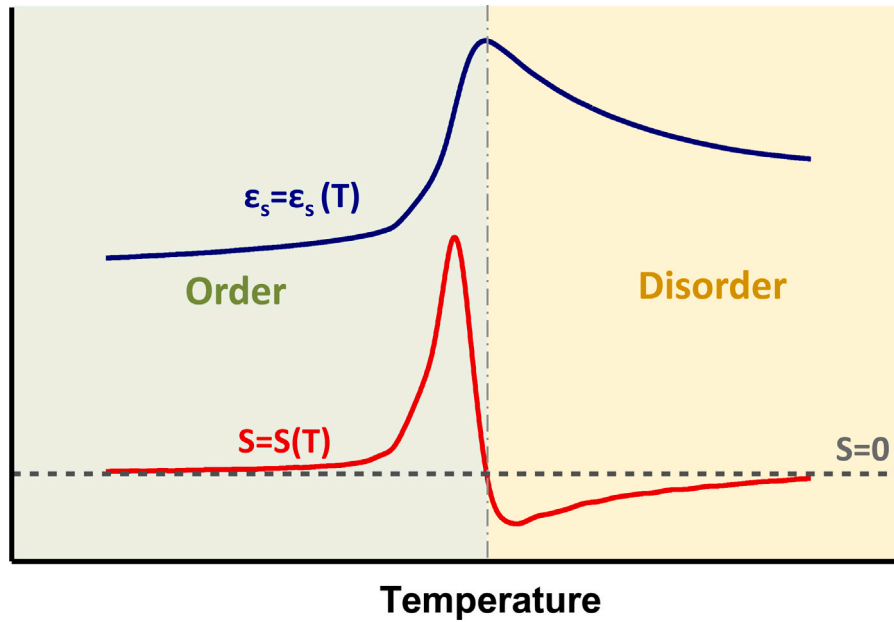


Fig. 1. Schematic temperature-dependence of the dielectric constant  $\epsilon_s$  (blue curve) and of the related entropy change as defined by Eq. (19b):  $S_E \propto \partial \epsilon_s / \partial T$  (red curve) due to the field-induced polarization. Fröhlich stated that if  $S_E > 0$  the field creates disorder, if  $S_E < 0$  it creates order. (For interpretation of the references to color in this figure legend, the reader is referred to the web version of this article.)

### Thermodynamic potentials of dielectrics: seminal relationships

Fröhlich equations give the relationships between electric field  $\mathbf{E}$ , dielectric displacement field  $\mathbf{D}$ , static dielectric function  $\epsilon_s$ , and total thermodynamic energy  $U$ , entropy  $S$ , Helmholtz free energy  $F$ . Fröhlich assumes that the considered material does not change in volume so, electrostriction effects can be neglected [33,35]. Then, when a reversible isothermal transformation is considered, the variation of these thermodynamic quantities can be written as

$$U(T, \mathbf{E}) = U_0(T) + U_E(T, \mathbf{E}), \quad (1a)$$

$$S(T, \mathbf{E}) = S_0(T) + S_E(T, \mathbf{E}), \quad (1b)$$

$$F(T, \mathbf{E}) = F_0(T) + F_E(T, \mathbf{E}), \quad (1c)$$

where  $U_0$ ,  $S_0$ ,  $F_0$  are the variation of respectively thermodynamic total energy, entropy, Helmholtz free energy at zero field, while  $U_E$ ,  $S_E$ ,  $F_E$  are their respective field-induced variations. The constraint of handling reversible transformations requires that, at each considered temperature, the involved physical variables are not time-dependent [71]. This means that relationships (1) should hold in static conditions only. In his treatise Fröhlich starts from the electromagnetic energy  $U_e$  of an ideal (loss-free) dielectric medium. So,  $U_e$ , for unit of volume, is given by

$$U_e = \frac{1}{2} \mathbf{E} \cdot \mathbf{D}. \quad (2)$$

If  $\mathbf{D}$  changes as a function of the temperature  $T$ , Eq. (2) will provide the energy variation (per unit volume) of the considered dielectric, although this relationship apparently does not include thermodynamic quantities. When the variation of  $\mathbf{D}$  is caused by some thermodynamic transformation, the effective energy  $U_e$  given by such expression will be dependent on the features of the occurring process. Becker pointed out that the change of electric energy  $dU_e$  coincides with the variation of the total thermodynamic energy  $dU$  in adiabatic conditions [36]. Conversely, in isothermal conditions,  $dU_e$  coincides with the change of the Helmholtz free energy  $dF$  [35,36]. It is worth noting that the volume variation of the system is here considered negligible, so the variations of Helmholtz and Gibbs free energies are the same. However, adiabatic experimental conditions are usually difficult to be handled [36]. Therefore, Fröhlich develops his theory in isothermal conditions, which can be much more easily theoretically managed.

Fröhlich considers a system whose volume is maintained constant and the sole independent variables are the temperature  $T$  and the external electric field  $\mathbf{E}$ . We summarize the conditions assumed by Fröhlich in four assumptions about the features of the dielectric, i.e.

1.  $\mathbf{D}$  linearly depends on  $\mathbf{E}$ ,
2. isotropic dielectric (scalar approximation),
3. ideal dielectric (loss-free medium),
4. negligible volume variation (no electrostrictions, etc.),

and two assumptions about the thermodynamics of the considered process, i.e.

1. reversibility,
2. isothermal conditions.

We here report the demonstration given by Fröhlich in his original texts [34,35]. All physical quantities were assumed for unit of volume, so we will in this exposition. We start from the assumed linear dependence  $D = \epsilon E$ ,<sup>7</sup> the scalar approximation ( $\epsilon$  is a scalar quantity) and the loss-free assumption (i.e.  $\epsilon$  is purely real). Moreover, no terms of volume variations will be considered. Fröhlich argument starts from the standard relationship which provides the density of electric energy  $u_e$  for unit volume of a dielectric material

$$u_e = \frac{1}{2} ED. \quad (3)$$

When a static field is considered, if the correlation between  $E$  and  $D$  is linear,

$$D = \epsilon_0 \epsilon_s E, \quad (4)$$

we have

$$u_e = \frac{1}{2} \epsilon_0 \epsilon_s E^2, \quad (5)$$

where  $\epsilon_0$  is the static vacuum constant and  $\epsilon_s$  is the relative static dielectric constant, as previously hinted. We stress that the requirement of considering an ideal dielectric implies that  $\epsilon_s$  is a purely real function. When  $\epsilon_s$  changes with the temperature  $T$ , Eq. (5) should provide

<sup>7</sup> We here employ the absolute dielectric function  $\epsilon \equiv \epsilon_0 \epsilon_s$ , where  $\epsilon_0$  is the vacuum dielectric permittivity and  $\epsilon_s$  is the static relative permittivity.

the energy difference (per unit volume) of the considered dielectric. From Eq. (3), we consider the quantity

$$du_e = \frac{1}{2} EdD, \tag{6}$$

which is the energy variation of the dielectric per unit volume when  $D$  is infinitesimally varied. If the change of  $D$  is due to some thermodynamic transformation occurring to the considered dielectric, the effective energy provided by the expressions (3) and (5) will depend on the features of the considered transformation. To discuss this, Fröhlich takes into account the two fundamental laws of thermodynamics: for an ideal system of volume  $v$  and pressure  $p$ , the first and second laws are respectively given, for a reversible transformation, by

$$dU = dQ - pdv, \tag{7}$$

$$dS = \frac{dQ}{T}, \tag{8}$$

where  $Q$  is the heat exchanged by the system,  $U$  is the exchanged energy,  $S$  is the entropy of the considered system, all calculated for volume unit. Here, we define the Helmholtz free energy  $F$  as

$$F = U - TS, \tag{9}$$

giving the maximum amount of work which can be extracted from a system in an isothermal process.<sup>8</sup> Eqs. (6) and (7) provide the energy variation  $dU$ , per unit volume, during a process where the field or the temperature, or both, are slightly varied:

$$dU = dQ + \frac{1}{2} EdD. \tag{10}$$

Such relationship has a structure similar to that of the state equation (7) where pressure and volume are replaced by  $-E$  and  $D$  respectively. Nevertheless, in Eq. (10) the dependence of  $D$  on temperature must be taken into account. When Eq. (4) holds, we obtain

$$dD = d(\epsilon_0 \epsilon_s E) = \epsilon_0 \left( \epsilon_s dE + E \frac{\partial \epsilon_s}{\partial T} dT \right),$$

which means that a change of  $D$  may be written as the sum of two contributions: a change in the field-strength  $E$  at constant temperature, and a change in temperature at constant  $E$ . Here, it is useful to employ  $T$  and  $E^2$  as the independent variables. So we write the first law of thermodynamics given by Eq. (10):

$$dU = dQ + \frac{1}{2} \epsilon_0 \epsilon_s d(E^2) + E^2 \epsilon_0 \frac{\partial \epsilon_s}{\partial T} dT = \frac{\partial U}{\partial(E^2)} d(E^2) + \frac{\partial U}{\partial T} dT. \tag{11}$$

A further relation is obtained from the entropy law, according to which  $dS$ , given by Eq. (8), is a total differential. This means that a unique function  $S = S(T, E^2)$  must exist such that

$$dS = \frac{\partial S}{\partial T} dT + \frac{\partial S}{\partial E^2} d(E^2). \tag{12}$$

Thus it is found that

$$dS = A(T, E^2) dT + B(T, E^2) d(E^2), \tag{13}$$

where  $A$  and  $B$  are both functions of  $T$  and  $E^2$ . The condition that  $dS$  is a total differential requires that

$$\frac{\partial B}{\partial T} = \frac{\partial^2 S}{\partial T \partial(E^2)} = \frac{\partial A}{\partial E^2}. \tag{14}$$

If we insert  $dQ$  from (11) into relationships (7) and (8), we will obtain

$$dS = \frac{1}{T} \left( \frac{\partial U}{\partial T} - \epsilon_0 E^2 \frac{\partial \epsilon_s}{\partial T} \right) dT + \frac{1}{T} \left( \frac{\partial U}{\partial(E^2)} - \frac{\epsilon_0 \epsilon_s}{2} \right). \tag{15}$$

<sup>8</sup> We recall that Fröhlich considers a system whose volume is maintained constant and the sole varying parameters are the temperature  $T$  and the electric field  $E$ .

This equation is of the type (13); therefore Eq. (14) becomes

$$\frac{\partial}{\partial T} \left[ \frac{1}{T} \left( \frac{\partial U}{\partial(E^2)} - \frac{\epsilon_0 \epsilon_s}{2} \right) \right] = \frac{\partial}{\partial(E^2)} \left[ \frac{1}{T} \left( \frac{\partial U}{\partial T} - \epsilon_0 E^2 \frac{\partial \epsilon_s}{\partial T} \right) \right],$$

whose differentiation gives

$$\frac{\partial U}{\partial(E^2)} = \frac{\epsilon_0}{2} \left( \epsilon_s + T \frac{\partial \epsilon_s}{\partial T} \right).$$

Integrating with respect to  $E^2$  yields the energy density

$$U = U_0(T) + \left( \epsilon_s + T \frac{\partial \epsilon_s}{\partial T} \right) \frac{\epsilon_0 E^2}{2}, \tag{16}$$

where  $U_0(T)$  is independent of  $E^2$  but depends on  $T$ , thus it represents the energy of the dielectric in absence of a field.

From these relationships, entropy  $S$  may be easily calculated: comparing Eq. (15) with Eq. (12), both  $\partial S/\partial T$  and  $\partial S/\partial(E^2)$  are known if  $U$  is introduced from Eq. (16). Thus

$$\frac{\partial S}{\partial T} = \frac{1}{T} \frac{\partial U_0}{\partial T} + \frac{\epsilon_0 E^2}{2} \frac{\partial^2 \epsilon_s}{\partial T^2},$$

$$\frac{\partial S}{\partial(E^2)} = \frac{\epsilon_0}{2} \frac{\partial \epsilon_s}{\partial T},$$

or integrating

$$S = S_0(T) + \frac{\epsilon_0 E^2}{2} \frac{\partial \epsilon_s}{\partial T}, \tag{17}$$

where  $S_0(T)$  is the entropy at zero field. From Eq. (9) one finally finds for the Helmholtz free energy

$$F = F_0(T) + \frac{\epsilon_0 \epsilon_s E^2}{2}, \tag{18}$$

where  $F_0(T)$  is the free energy in the absence of a field. We can summarize Fröhlich's results by saying that under the above-stressed assumptions, relationships (1) are expressed by

$$U(T, E) = U_0(T) + \frac{1}{2} \left( \epsilon_s + T \frac{\partial \epsilon_s}{\partial T} \right) E^2, \tag{19a}$$

$$S(T, E) = S_0(T) + \frac{1}{2} \frac{\partial \epsilon_s}{\partial T} E^2, \tag{19b}$$

$$F(T, E) = F_0(T) + \frac{1}{2} \epsilon_s E^2, \tag{19c}$$

which are the *Fröhlich's thermodynamic relationships* [35], i.e. respectively *Fröhlich total energy*, *Fröhlich entropy*, *Fröhlich free energy* (for unitary volume) [41,43,56]. We note that Relationships (19) point out that the usual expression (5) does provide the Helmholtz free energy only. Relations (19) have a transparent and simple mathematical form, being the free energy proportional to the dielectric function and the entropy proportional to its temperature derivative. Nevertheless, the elegant formulation of (19) requires the above-recalled specific hypotheses. We stress that the requirement of considering an independent-on-time field (static condition) is a consequence of the reversibility assumption. On the other hand, the dielectric assumptions concern the specific features of the dielectric response, which is determined by the considered material. Actually, in the present discussion the key physical quantity is the entropy, which, we write by combining Eq. (17) with Eq. (1b), i.e., in scalar approximation

$$S(T, E) = S_0(T) + S_E(T, E) = S_0(T) + \frac{1}{2} \frac{\partial \epsilon}{\partial T} E^2.$$

Therefore, the field dependent part of entropy is

$$S_E(T, E) = \frac{1}{2} \frac{\partial \epsilon}{\partial T} E^2. \tag{20}$$

Relationship (20) points out the *Fröhlich entropy* (FE), which can be seen as the entropy variation of the system due to the application of the electric field  $E$ , for volume unit [35]. We will see that, for practical uses, from Eq. (20) it is useful giving  $S_E(T)$  for a unitary field [41,56,57,72], i.e.

$$s(T) = \frac{1}{2} \frac{\partial \epsilon}{\partial T}. \tag{21}$$

$s(T)$  has the advantages of not depending on the strength of the electric field, featuring the structural information given by the dielectric response. Actually, Eq. (21) is the *key relationship* to exploit FE evaluation technique on the most of the physical systems.

*Generalized relationships: anisotropic and nonlinear dielectrics*

The constraints of linear and scalar dielectric response can be bypassed without specific assumptions on the physics of the considered material, but just through suitable mathematical treatments [26,30], which were recently developed by J. Parravicini [42]. We here report the final obtained relationships, without recalling the details of the calculations.<sup>9</sup>

*Anisotropic media*

If an anisotropic dielectric is assumed, the dielectric function must be expressed by a tensor  $\epsilon$ ; then  $\mathbf{D}$  as a function of  $\mathbf{E}$  has the form  $\mathbf{D} = \epsilon \cdot \mathbf{E}$ , i.e.

$$D_i = \sum_j \epsilon_{ij} E_j \tag{22}$$

for  $i, j = 1, 2, 3$ , where the components  $x, y, z$  of the field are  $E_x = E_1, E_y = E_2, E_z = E_3$ , and similarly for  $\mathbf{D}$ . So the generalized form of Eqs. (19) for anisotropic dielectrics is

$$U = U_0(T) + \frac{1}{2} \sum_{ij} E_j \left( \epsilon_{ij} + T \frac{\partial \epsilon_{ij}}{\partial T} \right) E_i, \tag{23a}$$

$$S = S_0(T) + \frac{1}{2} \sum_{ij} \left( E_j \frac{\partial \epsilon_{ij}}{\partial T} \right) E_i, \tag{23b}$$

$$F = F_0(T) + \frac{1}{2} \sum_{ij} (\epsilon_{ij} E_j) E_i. \tag{23c}$$

If we then focus on the entropy, from relationship (23b) we can evidently extend Eqs. (20) and (21) to the anisotropic case. So, Eq. (20) becomes

$$S_E(T) = \frac{1}{2} \sum_{ij} \left( E_j \frac{\partial \epsilon_{ij}}{\partial T} \right) E_i \tag{24}$$

and Eq. (21) will be

$$s(T) \equiv \frac{1}{2} \sum_{ij} \left( \frac{\partial \epsilon_{ij}}{\partial T} \right), \tag{25}$$

which have, of course, the same physical meaning of their corresponding formulae in the scalar case. We note that the expression (24) giving the field-induced entropy in an anisotropic medium is very similar to the usual expression giving the electric (free) energy density in the same conditions. This similarity can be highlighted by writing relationship (24) in the form

$$S_E(T) = \frac{1}{2} \frac{\partial \mathbf{D}}{\partial T} \cdot \mathbf{E}. \tag{26}$$

This last one can be immediately compared with Eq. (2), which we here write by underlining its dependence (through  $\mathbf{D}$ ) on temperature, i.e.

$$U_e(T) = \frac{1}{2} \mathbf{D} \cdot \mathbf{E}. \tag{27}$$

The physical meaning of relationships (23) can be pointed out by providing formulae (23) in the reference system of the principal axes [26], giving a diagonal  $\epsilon_{ij}$  tensor, i.e.

$$\epsilon_{ij} = \begin{pmatrix} \epsilon_{11} & 0 & 0 \\ 0 & \epsilon_{22} & 0 \\ 0 & 0 & \epsilon_{33} \end{pmatrix}. \tag{28}$$

<sup>9</sup> Of course, the hypotheses of considering an ideal dielectric and negligible volume variation and assuming the reversibility and isothermal conditions must still be valid.

Let us assume that the electric field is applied along the direction 1, where the system response is expressed by  $\epsilon_{11}$ , i.e.  $\mathbf{E} = (E_1, 0, 0)$ ; so, the corresponding entropy variation will be

$$S_E = S_{E_1} = \frac{1}{2} \frac{\partial \epsilon_{11}}{\partial T},$$

and analogously for a field along 2 and 3 directions. It is convenient expressing Eqs. (23) in polar coordinates, for the diagonalized system given by (28). If we are at a fixed temperature  $T$ , we will have

$$U_E(E, \theta, \phi) = \frac{E^2}{2} \left[ \left( \epsilon_{11} + T \frac{\partial \epsilon_{11}}{\partial T} \right) \sin^2 \theta \cos^2 \phi + \left( \epsilon_{22} + T \frac{\partial \epsilon_{22}}{\partial T} \right) \sin^2 \theta \sin^2 \phi + \left( \epsilon_{33} + T \frac{\partial \epsilon_{33}}{\partial T} \right) \cos^2 \theta \right], \tag{29a}$$

$$S_E(E, \theta, \phi) = \frac{E^2}{2} \left( \frac{\partial \epsilon_{11}}{\partial T} \sin^2 \theta \cos^2 \phi + \frac{\partial \epsilon_{22}}{\partial T} \sin^2 \theta \sin^2 \phi + \frac{\partial \epsilon_{33}}{\partial T} \cos^2 \theta \right), \tag{29b}$$

$$F_E(E, \theta, \phi) = \frac{E^2}{2} (\epsilon_{11} \sin^2 \theta \cos^2 \phi + \epsilon_{22} \sin^2 \theta \sin^2 \phi + \epsilon_{33} \cos^2 \theta), \tag{29c}$$

where  $E$  is the strength of the electric field. These relationships show that, if the electric field has strength  $E$  and direction given by  $\theta$  and  $\phi$  angles, when  $\epsilon_{ij}$  has the diagonal form (28), the components of the tensors  $(\epsilon_{ij} + T \partial \epsilon_{ij} / \partial T) / 2, (\partial \epsilon_{ij} / \partial T) / 2, \epsilon_{ij} / 2$  (at a given temperature) are the coefficients for calculating the values of the variations of the considered thermodynamic quantities. On the other hand, they can also be seen as the variation of total energy, entropy, free energy, respectively, due to the application of a unitary field along one of the principal directions of  $\epsilon_{ij}$  [26,41,56,57,72]. We stress that, if the components of  $(\epsilon_{ij} + T \partial \epsilon_{ij} / \partial T) / 2, (\partial \epsilon_{ij} / \partial T) / 2, \epsilon_{ij} / 2$  are known along the principal directions, relationships (29) will provide the values of the induced Fröhlich's total energy, entropy, free energy for a field with any  $\theta, \phi$  direction [26,29].

*Nonlinear media*

If the response of the dielectric to the field is not linear, second and third order nonlinear terms should be taken into account. So the field-dependent terms of (1) are written in the form

$$U_E = U_E^{(1)} + U_E^{(2)} + U_E^{(3)}, \tag{30a}$$

$$S_E = S_E^{(1)} + S_E^{(2)} + S_E^{(3)}, \tag{30b}$$

$$F_E = F_E^{(1)} + F_E^{(2)} + F_E^{(3)}, \tag{30c}$$

where  $U_E^{(1)}, U_E^{(2)}, U_E^{(3)}$  are the terms depending on linear, quadratic, and cubic dielectric responses, respectively, and analogously for entropy and Helmholtz free energy.

The fundamental relation between  $\mathbf{D}$  and  $\mathbf{E}$  (Eq. (22)) are expressed by

$$D_i = \sum_j \epsilon_{ij}^{(1)} E_j + \sum_{jk} \epsilon_{ijk}^{(2)} E_j E_k + \sum_{jkl} \epsilon_{ijkl}^{(3)} E_j E_k E_l, \tag{31}$$

where  $\epsilon_{ij}^{(1)} = \epsilon_{ij}$  of the linear anisotropic case (22),  $\epsilon_{ijk}^{(2)}$  and  $\epsilon_{ijkl}^{(3)}$ , for  $i, j, k, l = 1, 2, 3$ , are respectively the absolute second- and third-order nonlinear dielectric functions. The expression of the total energy, in the form of (1a), for a nonlinear medium is

$$U = U_0(T) + \frac{1}{2} \sum_{ij} \left( \epsilon_{ij}^{(1)} + T \frac{\partial \epsilon_{ij}^{(1)}}{\partial T} \right) E_i E_j + \frac{1}{3} \sum_{ijk} \left( \epsilon_{ijk}^{(2)} + T \frac{\partial \epsilon_{ijk}^{(2)}}{\partial T} \right) E_i E_j E_k +$$

$$+ \frac{1}{4} \sum_{ijkl} \left( \epsilon_{ijkl}^{(3)} + T \frac{\partial \epsilon_{ijkl}^{(3)}}{\partial T} \right) E_i E_j E_k E_l, \quad (32)$$

while the entropy

$$\begin{aligned} S = S_0(T) &+ \frac{1}{2} \sum_{ij} \left( \frac{\partial \epsilon_{ij}^{(1)}}{\partial T} \right) E_i E_j + \\ &+ \frac{1}{3} \sum_{ijk} \left( \frac{\partial \epsilon_{ijk}^{(2)}}{\partial T} \right) E_i E_j E_k + \\ &+ \frac{1}{4} \sum_{ijkl} \left( \frac{\partial \epsilon_{ijkl}^{(3)}}{\partial T} \right) E_i E_j E_k E_l, \end{aligned} \quad (33)$$

and the Helmholtz free energy:

$$\begin{aligned} F = F_0(T) &+ \frac{1}{2} \sum_{ij} \left( \epsilon_{ij}^{(1)} \right) E_i E_j + \\ &+ \frac{1}{3} \sum_{ijk} \left( \epsilon_{ijk}^{(2)} \right) E_i E_j E_k + \\ &+ \frac{1}{4} \sum_{ijkl} \left( \epsilon_{ijkl}^{(3)} \right) E_i E_j E_k E_l. \end{aligned} \quad (34)$$

These last relations have the form of (1) and their parts dependent on field have the form of (30). They are the Fröhlich relationships for a material with both second- and third-order nonlinearities. The scalar formulation of (32), (33), and (34) can be useful for highlighting their physical meaning. It is

$$\begin{aligned} U = U_0(T) &+ \frac{1}{2} \left( \epsilon^{(1)} + T \frac{\partial \epsilon^{(1)}}{\partial T} \right) E^2 + \\ &+ \frac{1}{3} \left( \epsilon^{(2)} + T \frac{\partial \epsilon^{(2)}}{\partial T} \right) E^3 + \frac{1}{4} \left( \epsilon^{(3)} + T \frac{\partial \epsilon^{(3)}}{\partial T} \right) E^4, \end{aligned} \quad (35a)$$

$$S = S_0(T) + \frac{1}{2} \frac{\partial \epsilon^{(1)}}{\partial T} E^2 + \frac{1}{3} \frac{\partial \epsilon^{(2)}}{\partial T} E^3 + \frac{1}{4} \frac{\partial \epsilon^{(3)}}{\partial T} E^4, \quad (35b)$$

$$F = F_0(T) + \frac{1}{2} \epsilon^{(1)} E^2 + \frac{1}{3} \epsilon^{(2)} E^3 + \frac{1}{4} \epsilon^{(3)} E^4. \quad (35c)$$

These equations point out that a not-null second-order nonlinearity makes the thermodynamic quantities depending on the cube of the applied field: this indicates that a dielectric system with  $\epsilon^{(2)} \neq 0$  is necessarily not-centrosymmetric, highlighting that a material with a not-null static second-order nonlinearity must host a symmetry-breaking.

### Physical meaning of Fröhlich entropy

We here examine three different meanings of Fröhlich entropy. The *first* one is correlated with the simplest model of a dielectric, i.e. a set of dipoles that may be oriented by a measuring field. The *second* one stresses that FE can be used to check the state-of-order of a system; namely, it is found very useful to describe the features of phases and correlated transition processes. The *third* framework highlights the capability to give a measure of the stability within an explored phase. All these views have been practically exploited in the investigation of physical systems where FE evaluation has been carried out. It is worth noting that the original previously quoted Fröhlich's interpretation<sup>10</sup> was also recalled e.g. by Scaife and by Böttcher, with similar sentences, in their classical monograph on dielectrics [38–40].<sup>11</sup>

#### Fröhlich entropy as a figure of merit of orientation disorder

The relationships involving  $U$ ,  $S$ , and  $F$  exposed in the previous sections have deep physical meanings. In fact, Eq. (18) for the free energy shows that the amount of electric energy available in an isothermal

reversible process is  $\epsilon_0 \epsilon_s E^2/2$ . Through Eq. (16), on the other hand, Fröhlich demonstrates that substances following the Curie–Weiss law, such as e.g. diluted dipolar gases, the temperature dependent part of  $\epsilon_s$  does not provide any contribution to the total energy [35].<sup>12</sup>

For this treatise, the most important results involve the entropy as given by Eq. (20). It shows that the entropy of the considered system is increased by the field if  $\partial \epsilon_s / \partial T$  is positive, while it is decreased when this quantity is negative. We follow the original Fröhlich's rationale, which was exposed in the above-quoted sentences from [35]. Let us consider a physical system with dipoles being free-to-reorient, such as liquids and gases. In these conditions  $\epsilon_s$  decreases with increasing  $T$  [59]: here, an external field forces the dipoles to coherently reorient, so creating ordering. This may be expected because the field will orientate some of the dipoles which in the absence of a field are at random. Conversely, if we consider a system where inherent dipoles are in a well ordered state – such as typically found in a crystalline solid – here they lie in stable energy minima. The correlated trend of  $\epsilon_s$  is to increase with  $T$ . This means that an external field increases the disorder. Namely, effect of the field is to perturb a (relatively) stable configuration by turning some of the dipoles into different directions, so the field can only decrease the existing order. Therefore FE can be considered as a measure of the orientation freedom degree, i.e. an *orientation entropy*, providing information about the rearrangement of the electric dipoles which belong to the system [33,73,74]. An ideal behavior of  $\epsilon(T)$  and the correlated  $S_E(T)$  are depicted in Fig. 1, which reproduces the scheme in the original Fröhlich's treatise. Of course, this picture is not limited to specimens hosting permanent dipoles (e.g. polar liquids [33,59]), but it can be applied to all samples where the internal charge distribution can be suitable approximated to dipolar terms, at least at the first order. It means that this physical interpretation holds for a great part of the condensed matter: actually, in his treatise Fröhlich provides this interpretation in a very general and concise way. However, we recall that the above-mentioned hypotheses about the thermodynamic equilibrium, static conditions (no time dependent fields [59,75]) and the suitable constitutive relationships between  $E$  and  $D$  (or  $P$ ) are key factors. We stress that when the imaginary part of the dielectric response is not negligible, i.e. strong time relaxation phenomena are present [18–21], the recalled Fröhlich's arguments cannot be employed, so the here discussed experimental approach cannot be used. This implies that dielectric loss tangent  $\tan \delta \equiv \text{Im}(\epsilon) / \text{Re}(\epsilon)$  can be approximated to 0 or, in terms of practical dielectric spectroscopy, the condition

$$|\tan \delta| \ll 1 \quad (36)$$

holds [16]. The strength of  $E$ , on the other hand, should be carefully handled, because when very high fields are applied (typically  $\geq 10^4$  V/cm), the system can be strongly perturbed and  $E$  can affect not only the orientation of the internal dipoles, but their structure also (coercive field effects) [15,16,19,59]. Differently, the probing electric field employed in the here discussed experiments is typically  $\lesssim 5$  V/cm.

#### Fröhlich entropy: a convenient state-of-order indicator

We want here to emphasize that Fröhlich entropy can be fruitfully exploited to finely describe the state-of-order of a macroscopic system, in absence of important time relaxation phenomena.<sup>13</sup> Moreover, since FE derives from dielectric measurements, practically it allows to almost continuously follow the evolution on temperature of the order state, which signals the features of the considered phase and correlated transitions. Namely, the powerful of FE evaluation is particularly evident when phase transitions occur. Actually, an order/order transition

<sup>12</sup> Pg. 12 §3, Eqs. (3.11) and (3.14) of Ref. [35].

<sup>13</sup> I.e. under the above-recalled Fröhlich's hypotheses on equilibrium and not-time-dependent fields.

<sup>10</sup> Section “Introduction and landscape”.

<sup>11</sup> See, in particular, chapter 3 §13 of [38].

manifests itself as a variation of the positive level of the  $S_E$  curve, since the entropy contribution supplied by the field is positive both before and after the transition. The corresponding values of  $S_E(T)$  are in agreement with the degree of order of each phase [35,40,44,52,53]. In the transition interval, a characteristic peak can be found, whose width can be assumed to estimate the temperature extension of the transition process. An analogous behavior, with negative  $S_E(T)$  values, can be displayed in the case of a disorder/disorder transition. On the other hand, when an order/disorder transition occurs, a two-opposed-peaks lineshape of  $\partial\epsilon_r/\partial T$  is typically displayed (Fig. 1), in correspondence with the positive and negative slope in the related permittivity peak, with negative part marking a disordered state in the material. Therefore, the estimation of FE is demonstrated to be a particularly sensitive probe for investigating phase transition phenomena. These features can be found in a very large class of systems.

#### Fröhlich entropy: a quantitative evaluation of phase stability

FE was also demonstrated to be able to provide specific information about the stability of a considered long-range phase. This conceptual approach was developed mainly in works concerning organic molecular crystals [52,53]. This concept starts from the above recalled Fröhlich's interpretation (Section "Fröhlich entropy as a figure of merit of orientation disorder"). When an electric field is applied, if the corresponding value of  $|S_E(T)|$  is great, this implies that the system is strongly modified by the application of  $E$ . On the other hand, if the corresponding value of  $|S_E(T)|$  is relatively small, this means that  $E$  slightly changes the status of the system. Then, we can reasonably assume that, in the considered conditions, the system in the first case is in a less stable configuration than in the second case. So, both for ordered ( $S_E > 0$ ) and disordered ( $S_E < 0$ ) configurations, FE is able to provide an immediate quantitative estimation of the stability of a given temperature dependent phase and to compare this feature between different phases. In particular, a nearly constant trend of  $S_E(T)$  points out a temperature region with highly stable features, while a steeply changing of  $S_E(T)$  is associated to instability features, which typically become the most marked in correspondence to the phase transition temperature regions.

The scheme in Fig. 1 can be useful to grasp this physical picture. We can see that the greatest values of  $|S_E(T)|$  correspond to the region around the phase transition, where the system configuration is reconfiguring and its long-range state is highly unstable. As more as it moves away from the transition, the phase is stabilizing, so the applied electric field only negligibly perturbs the system [19]: this is pointed out by the small values of  $|S_E(T)|$ , which are decreasing slower and slower where a long-range phase is achieved. Moreover, a further signature of phase instability is given by the arising of oscillations of  $S_E(T)$  as a function of temperature (see e.g. Fig. 15b below), where a regular (nearly constant) trend of FE (see e.g. Fig. 14 below) is instead a clear signal of a highly stable and not changing phase [52,53]. Further signatures of instability phenomena are the presence of oscillations of  $S_E(T)$  [52], showing that the dipoles of the considered system are quickly reconfiguring. In particular, when these oscillations cross the  $S_E = 0$  value, the presence of oscillations signals the arising of hybrid and metastable phases, where order and disorder coexist. There, the order degree of the system is reconfiguring, rapidly passing from disordered to ordered state, or it is not well defined (Fig. 2).

#### Investigation of physical systems by using Fröhlich entropy

##### General view

The generality of the relationship that defines Fröhlich entropy and the use of his interpretation in studying very different physical systems raise the problem of practically satisfying its theoretical validity conditions, whose assumptions are listed in Section "Thermodynamic

potentials of dielectrics: seminal relationships". These guarantee that the formalism of relation (19b) (and its extensions (33) and (23b)) holds. Experiments demonstrated that Fröhlich entropy relationship can be applied in less stringent conditions with respect to the formal ones. Namely, relationship (19b) was experimentally found to hold in quasi-equilibrium states [41,52,53] and quasi-static conditions [44–46,62], i.e. they still hold when relaxation phenomena are negligible: this implies that quasi-static fields (frequencies until  $\approx 100$  MHz [47]) can be handled provided that the condition (36) still holds. On the other hand, the validity of hypotheses on dielectric features strongly depends on the investigated material: namely, the isotropy assumption of Fröhlich discussion can be not assumed, so the investigation of systems whose response is intrinsically directional is also possible. In fact, it has been accomplished on anisotropic crystals [41,56,72] and nematic compounds [47–50,76], also before the mathematical formulation of the anisotropic extension of Fröhlich's original relationship [42], which are here reported in Eqs. (33) and (23b). Although the extension of Eq. (19b) to nonlinear dielectric response has been already provided (i.e. high electric field conditions), no experimental works explicitly involving the estimation of FE in nonlinear regimes has been up today already carried out.

We here provide a comprehensive landscape of the physical systems where FE has been employed as an investigation instrument aimed at gaining specific information about material state and its evolution. We will not discuss investigations where, although Fröhlich relationships are used, experimental conditions determine that the application of the electric field not negligibly modify the structure of the considered physical system. In other words, we will consider those works where the applied  $E$  can be considered a *probing field*. For this reason, we will not discuss the works of the groups of e.g. G. Johari and R. Richert about structural polar and glassy liquids, where relationships involving FE are employed for describing structural changes induced by the application of the electric field [18,19,33,59–62,77].

First we will consider the investigation of phase transitions and melting processes in confined metallic Ga nanoparticles. They are the first system where FE evaluation has been systematically exploited for interpreting experimental results by GB. Parravicini et al. of Pavia group in 2003 [44–46]. Then, we will discuss systems of polar liquids and glasses, where FE has been employed in several works since 2007, mainly due to J. Jadzyn et al. of Poznań group. Subsequently, the use of FE for analyzing phase transitions and phase stability in semiconductor molecular crystals is considered. Fröhlich's argument has been fruitfully used in the investigation of disordered ferroelectric crystals also, whose evolution of the order state has been finely described and a directional description has been remarkably provided. Finally, works on FE in polymeric films and diluted enzymes will be discussed.

##### Confined metallic nanoparticles

As hinted before, the first class of physical systems where the Fröhlich formalism was applied in the interpretation of experimental results are confined metallic nanoparticles. Specifically, Ga nanoparticles embedded in a  $\text{SiO}_x$  matrix are considered, a paradigmatic arrangement analogous to other confined systems where the interfaces play a key role [78,79].

The issue of phase transitions in nanometric-size metallic particles studied through dielectric spectroscopy had been faced in a preliminary work by Pavia group in 2000 [80]. The investigation of Ga was considered a very interesting topic due to the rich polymorphism of this element; actually, several investigations gave the evidence of the existence, in submicrometer particles, of different metastable structural phases (named  $\beta$ ,  $\gamma$ ,  $\delta$ , and  $\epsilon$ ) [78,79,81–83]. The main result of this experimental work was the assessment of hysteresis loop crossing melting and solidification temperatures. This investigation, moreover, demonstrated that the employed dielectric technique was able to inspect the various solid phases of the confined Ga nanoparticles [80].

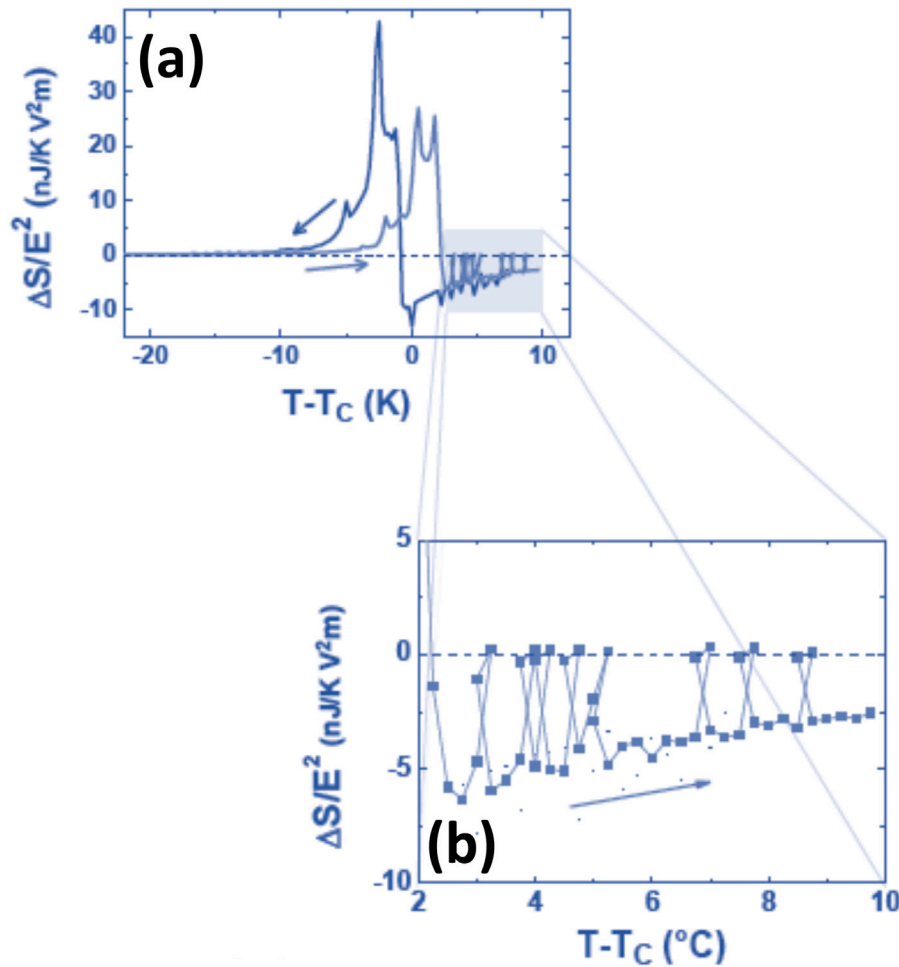


Fig. 2. (a) Fröhlich entropy ( $S_F$  is here indicated with  $\Delta S$ , per volume unit, normalized to the squared probe-field amplitude  $E^2$ ) in proximity of the Curie point of a disordered potassium-based perovskite crystal and (b) blow-up of shaded region illustrating phase fluctuations from liquid-like to solid in the heating stage. Source: Adapted from Supplementary Information of [55], Fig. 2.

After this work, a specific effort was accomplished towards getting more information about the nanoparticle phase evolution from dielectric measurements. Hence, a new analysis approach exploiting Fröhlich’s theory and interpretation was given in 2003, in a work where melting and premelting processes are investigated “through capacitance measurements” [44]. The Fröhlich’s interpretation was more specifically applied in the following works, where the temperature evolution of the “degree of order” [46] and the temperature-dependent order–disorder changes [45] are analyzed. In these works the capacitance measurements on metallic nanosystems are proved to give detailed information on the phase transitions and the correlated premelting and melting processes, with their dependence on sizes of involved particles [44–46,84].

In these works the investigated samples containing Ga particle layers are considered as a system of two capacitors in series, the layer of  $\text{SiO}_x$  and the layer of Ga clusters, as shown in Fig. 3 [85]. The capacitance contribution of the Ga layers was extracted and its derivative  $dC(T)/dT \propto S_F(T)$  (proportional to FE, Eq. (19b)) was calculated.

Phase transitions

The features of phase transitions are investigated on two different samples of Ga nanoparticles, whose the most representative are particles of 20 nm radius (Ga20). Preliminary transmission electron microscope (TEM) measurements as a function of temperature, reported in Fig. 4, point out in Ga20 sample a solid–liquid transition of the

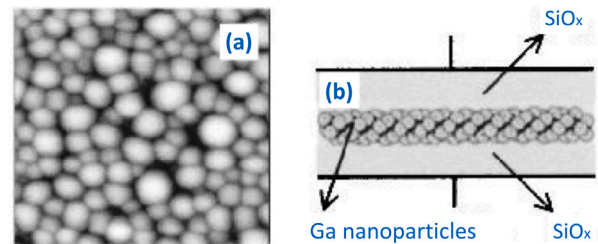
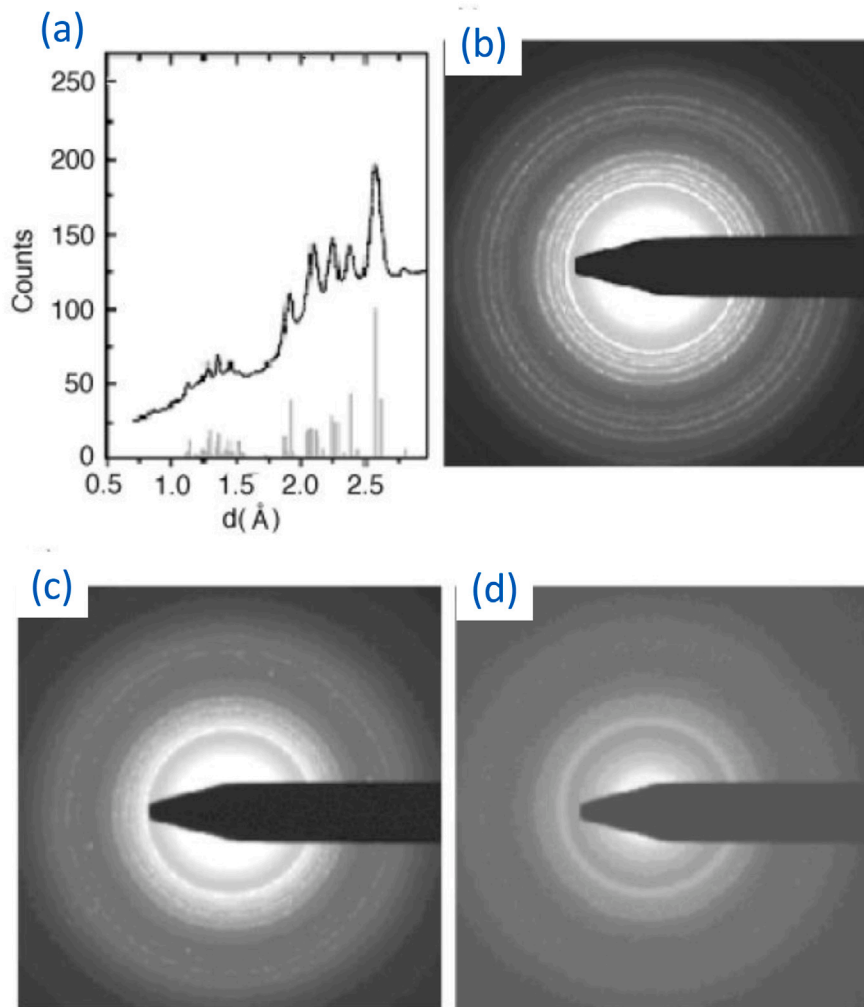


Fig. 3. Typical sample arrangement of the works on Ga confined nanoparticles here considered. (a) AFM plain-view image of the Ga nanoparticles arrays in sample; (b) schematic representation of the sequence  $\text{SiO}_x/\text{Ga nanoparticles layer}/\text{SiO}_x$ . Source: Adapted from [85], Fig. 1.

Gallium at the temperature  $T_c = 250 \text{ K}$  [46]. Specifically, the crystalline phase in solid state is identified by TEM as  $\delta$ -phase displaying trigonal structure, in very good agreement with the data reported in literature. Remarkably, when the detected transition from solid to liquid phase is considered, the melting process is found to start about 65 K below the full melting temperature value.  $\epsilon = \epsilon(T)$  evolution is plotted in Fig. 5: both real and imaginary part of the measured dielectric function show the occurrence of a transition centered at 185 K. It is worth stressing the high sensitivity of such a kind of measurements: actually the corresponding electronic diffraction measurements (Fig. 4) are able to detect hints of a transition only at 240 K and its end at 250 K.





**Fig. 4.** TEM measurements — (a) Ga  $\delta$  phase: selected area of electronic diffraction (SAED) radial plot of Ga clusters in the solid phase. In the upper part of the figure the calculated diffraction pattern of the Ga  $\delta$  phase is reported. (b) The correspondent SAED pattern. The SAED patterns in (c) 240 K and (d) 250 K, respectively, giving evidence of solid-liquid phases and full liquid phase are reported.

Source: Adapted from [46], Fig. 3.

FE correlated to the dielectric response of Fig. 5 is reported in Fig. 6, where it is given in terms of derivative of the dielectric capacitance  $C = C(T)$  as a function of the temperature:  $dC/dT \propto S_E \propto \partial\epsilon/\partial T$ . Plot of Fig. 6 highlights that the change from a positive to negative value of  $dC/dT$  corresponds to a transition from an ordered phase to a disordered one, i.e. from the solid to a liquid state of Ga. In particular, the trend of FE vs. temperature demonstrates that the disorder of the system increases with  $T$  until 250 K. We note that the presence of a slope change at 220 K signals the arising of pretransitional features, while the occurring of the specific transition is abruptly pointed out by the change of sign at 185 K. As an apt conclusion of these studies, a comprehensive EXAFS investigation on Ga nanoparticles accurately confirmed the polymorphism and pretransitional effects highlighted by dielectric measurements and FE analysis [86].

#### Melting processes

We here discuss more deeply the specific item of melting process. As we hinted before, in low-size systems the amount of surface atoms with respect to the bulk ones cannot be considered negligible, so the melting processes in such systems display peculiar features. In these conditions the use of FE analysis, which gives the possibility of continuously following the evolution vs. temperature, enables to carry out a detailed study. This topic was specifically faced in two works about the melting evolution in Ga nanoparticles [44,46].

Among the order/disorder phase transitions, melting is one of the most extensively observed, but achieving a complete microscopic description often is difficult. For instance, it is well known that in the considered Ga metallic nanoparticles thermodynamic properties related to melting show significant deviations with respect to the bulk ones. The key role of the surface in the melting processes was stressed in different experimental investigations [87,88]. By means of optical, Dark Field Electron Microscopy (DFEM) and electronic microscopy (TEM) techniques on metal nanoparticles evidence was given of premelting processes, namely the formation of a liquid layer, some degrees below the complete melting, that progressively expands with increasing  $T$  (Fig. 4). Melting precursor effects specifically involving the first surface atom layers were investigated (surface pre-roughening, roughening, reconstruction) [89]. This is particularly relevant in the nano-size scale, where the role of surfaces and interfaces becomes predominant [90]. Carried out measurements highlight the occurrence of surface changes as a thin molten layer around the solid core which arises some degrees before full melting. This is due to the interplay of the involved interface quantities  $\gamma_{sm}$ ,  $\gamma_{sl}$ ,  $\gamma_{lm}$ , i.e. the free energies per unit area of solid-matrix (sm), liquid-matrix (lm) and solid-liquid (sl) interfaces respectively. The melting happens when the inequality  $\gamma_{sm} - \gamma_{sl} - \gamma_{lm} > 0$  holds. In Ga nanoparticles, when TEM investigation is accomplished, above-shown SAED pictures and spectra point out a complete bulk melting of the embedded nanoparticles between 240 and 250 K (Fig. 4). Conversely,

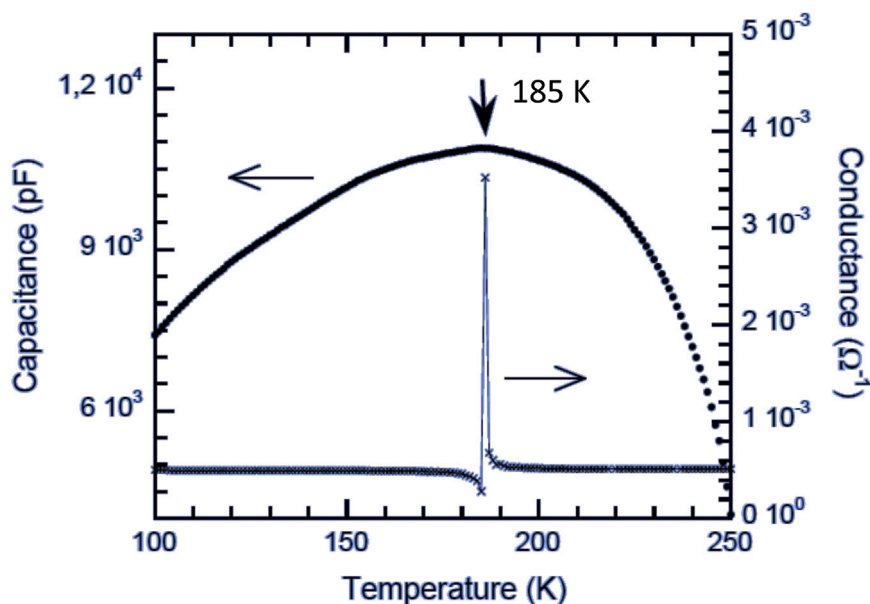


Fig. 5. 20 nm size sample: capacitance and conductance of the Ga nanoparticles layer as a function of temperature in the range below the full melting temperature. Source: Adapted from [45], Fig. 3.

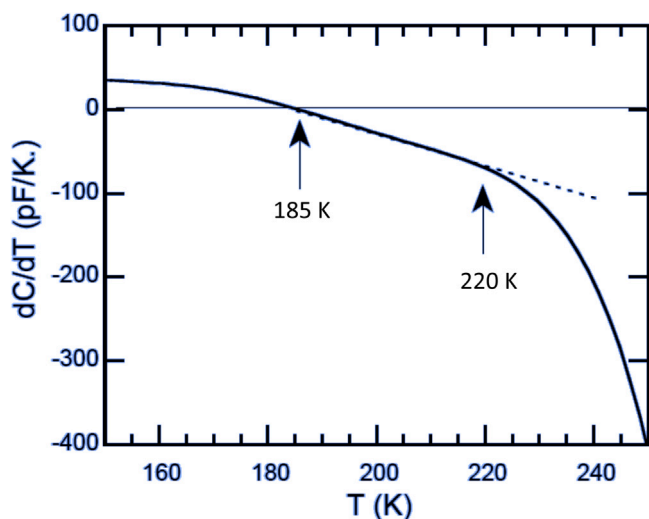


Fig. 6. Derivative of the Ga layer capacitance  $C$  of Fig. 5 as a function of the temperature  $T$ , vs. temperature (solid line). The derivative is proportional to the entropy due to the applied field. The change of sign, at  $T = 185$  K, points out an order–disorder transition. The dotted line shows a linear behavior in the 185–220 K interval showing the progressive disorder increasing of the atoms before inner melting starting at 220 K.

Source: Adapted from [45], Fig. 4.

FE analyses are found to be able to specifically detect surface precursor phenomena. Actually, the dielectric response is closely related to the polarized surface of the nanoparticles: this implies that such a technique selectively gets the signal of first atomic layers of the considered physical system.

Fig. 6 displays the derivative of  $C(T)$ , which is  $dC(T)/dT \propto S_E(T)$ . The plot clearly points out the sign change at 185 K, assessing the onset of an order–disorder transition. In the interval 220–250 K we compare TEM images with FE analysis results. These are characterized by a progressively more pronounced slope, as one expects, when the instabilities are strongly enhanced and start involving the inner part of the system [35,44,46]. In this temperature interval, when inner melting is occurring, the slope manifests a clear divergence. In Fig. 6 a linear

slope is observed in the  $T$ -range 185–220 K, where TEM data are not modified by any  $T$ -dependent process. The data can be interpreted in terms of onset of vibrational instabilities at the very surface before reaching the critical value. This value is predicted for melting by the Lindemann criterion, expressed by the Lindemann ratio,  $\delta_L$ , i.e. the ratio between the root-mean-square displacement,  $\delta L$  rmsd, of a particle from its equilibrium position to the distance between them. It is worth noting that the presence of two regimes had been predicted in a similar context by molecular dynamic (MD) simulations performed on a nanosystem made of 6912 (a size comparable to metallic nanoparticles here investigated) obeying Lennard-Jones potential and overheated using appropriated step-by-step procedures [87,88]. In this vein, it is illuminating to compare Fig. 6 with Figs. 7 and 8 (from [87]): the entropy divergence compares nicely to the divergence of Lindemann disordered atoms vs. temperature. The linear slope of the FE variation from 185 K to about 220 K can be related to the linear increase of the rmsd of (surface) atoms before reaching the inner melting region (see Figs. 7 and 8), in strict agreement with [87]. We stress that the very high specific sensitivity to the local surface atoms evolution of the dielectric measurements allows us to monitor the different stages of pre-melting and full melting processes in a wide temperature region. The existence of two regimes pointed out in the  $dC/dT$  trend is an important result illustrating the potential of the employed method.

### Summary

Summarizing, the investigation of phase transitions on Ga nanoparticles shows that the FE evaluation method is particularly sensitive to the evolution of the low-sized (less than  $\mu\text{m}$ ) systems, where the surface features are a key ingredient to produce melting and, more generally, phase transition processes. The relationships given by Fröhlich between dielectric function and entropy is demonstrated to be useful in investigating surface phenomena in these nanometric systems in terms of order–disorder transitions and their evolution. The FE estimation, although it is an intrinsically macroscopic measurement, is found to be very accurate in describing the dynamics of surface atoms, allowing to follow the different phases of premelting and full melting. Therefore, the investigation of melting processes by dielectric measurements and related FE estimation was demonstrated to display the strict correlation of the dielectric response with the surface polarization, notably the surface first atomic layers and a high sensitivity for finely following the phase transition evolution.

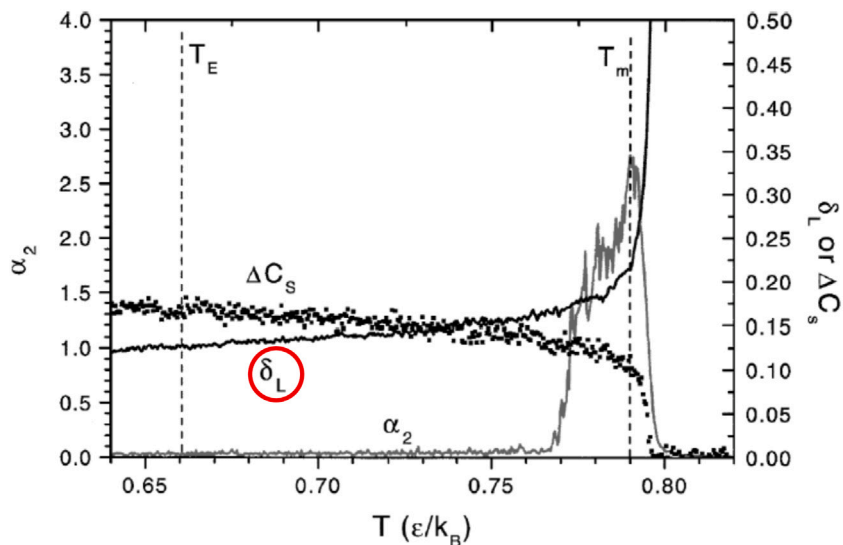


Fig. 7. The experimental Lindemann parameter ( $\delta_L$ ), the effective shear modulus  $\Delta C_S$  (squares), and  $\alpha_2$  parameter versus temperature. Source: Adapted from [87], Fig. 2.

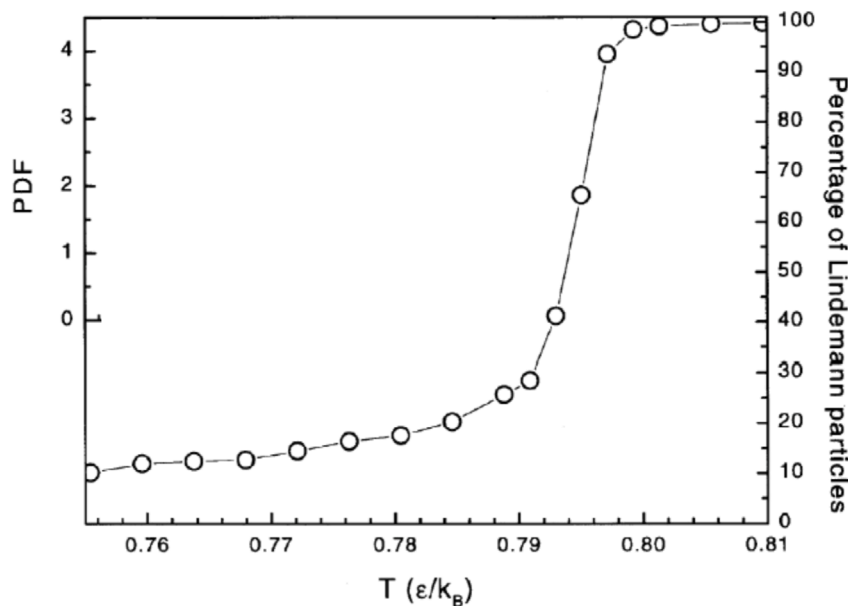


Fig. 8. Calculated percentage of Lindemann particles as a function of temperature as also reported by [88]. Source: Adapted from [87], Fig. 3.

**Polar liquids and glasses**

Further wide classes of materials where FE interpretation was demonstrated to be a useful experimental tool is that of polar liquids and glasses. Frohlich’s relationships were used to describe both structural liquids and nematicons, in a series of works mainly carried out by J. Jazdyn and his group.

**Structural liquids and glasses**

FE evaluation is exploited to describe the arrangement of structural liquids, both organic and inorganic, in suitable solvents. Studies are carried out on polar inorganic pure formamide [91], propylene carbonate and dimethylsulfoxide (DMSO) with their mixtures [92], highly-polar amide compounds such as n-methylpropionamidine, its homologue n-methylacetamide, and n-ethylacetamide [74], organic lactones [93], inorganic lithium perchlorate in polyethylene glycols solvent [94]. On a different research line, a theoretical study of D.V. Matyushov et al.

takes into account the configurational entropy of several polar organic liquids undergoing glass transition [58].

A meaningful example of such a kind of studies is reported in Fig. 9, where the FE behavior of n-methylpropionamidine (NMP) and n-ethylacetamide (NEA) is depicted [74]. It is calculated by the relationship:

$$\frac{\Delta S}{E^2} = \frac{S(E, T) - S_0(T)}{E^2}, \tag{37}$$

where  $\Delta S$  is the entropy variation for unit of volume which is due to the application of the electric field<sup>14</sup>, so  $\Delta S/E^2$  is  $s$  of Eq. (21). Here FE evaluation is exploited to obtain information on the intermolecular interactions and the molecular self-aggregation abilities of the considered liquids. The plot in Fig. 9b shows, for all the studied compounds, that

<sup>14</sup>  $\Delta S$  of Eq. (37) is the same quantity of  $S_E$  in Eq. (20)

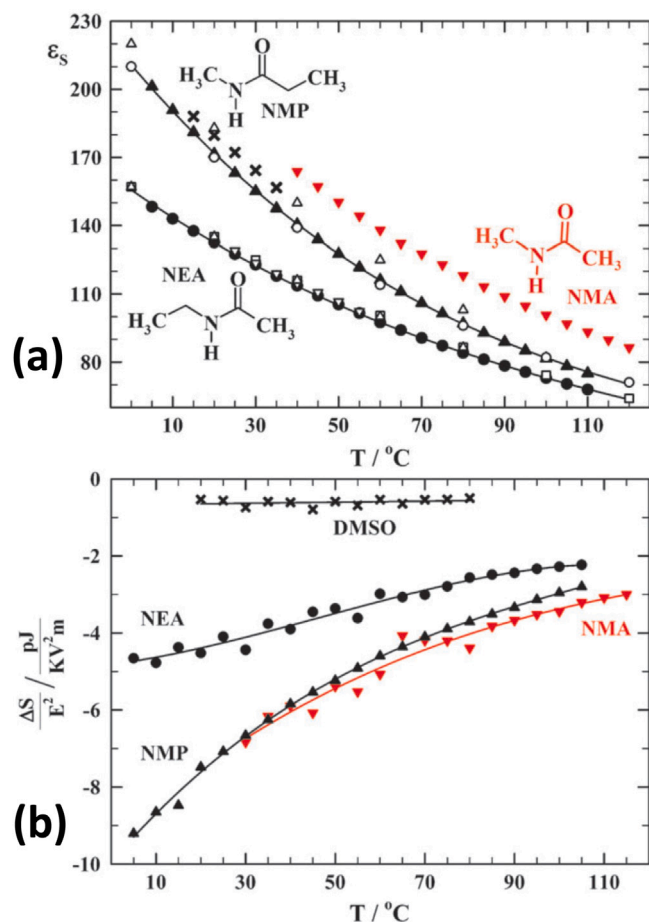


Fig. 9. (a) static dielectric permittivity of n-methylpropionamide (NMP), n-ethylacetamide (NEA) as a function of  $T$ , experimentally obtained in [74] (full points) and the literature data. Permittivity data for n-methylacetamide NMA are also depicted for comparison. (b) corresponding orientational entropy variation for n-methylpropionamide (NMP), n-ethylacetamide (NEA) and n-methylacetamide NMA. Data for dimethylsulfoxide (DMSO) are also reported for comparison.

Source: Adapted from [74], Figs. 9 and 10.

the FE is negative, as we expect for a disordered dipolar liquid, where an applied field creates order. When the temperature is increased, the lowering of the modulus of the induced negative entropy gives a measure of the progressive decrease of the disorder in the samples. Actually, the authors associate this response to the formation of multimolecular aggregations which continuously increase their order. The comparison with the trend of non-self-associated compounds such as DMSO, whose FE is constant vs. temperature, confirms that FE response describes these peculiar behavior of the dipolar molecules [74].

Such experimental approach was also used to specifically highlight the variation of orientational features as a function of solvent concentration: this was carried out, as hinted above, with mixtures of propylene carbonate and DMSO, a compound of significant application interest [92]. The plot of Fig. 10 shows FE dependence on both temperature and solvent concentration  $x_{\text{DMSO}}$ . It allows to follow the structural evolution of the physical system with a crossed-view between stoichiometry and temperature.

#### Nematic solutions

A further set of compounds where FE evaluation is fruitfully employed is liquid crystals. In particular, this approach was used in 2008 to describe the dynamics of mesogenic 4-(trans-4'-n-hexylcyclohexyl)isothiocyanatobenzene molecules in prenematic conditions [95]. Notably, the authors claimed that this work, and other of the same

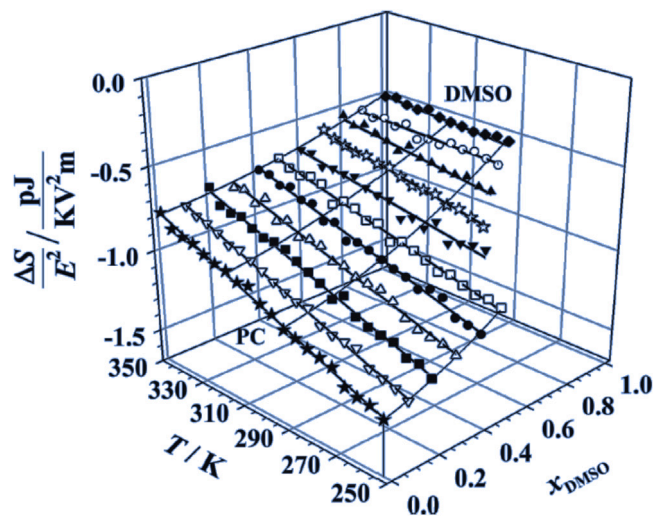


Fig. 10. FE for mixtures of propylene carbonate and DMSO of different compositions at different temperatures.

Source: Adapted from [92], Fig. 5.

group [47,76,96], were the first to experimentally exploit Fröhlich equations and interpretation, although the previously discussed works on Ga nanoparticles had been published four years before [44–46], Section “Confined metallic nanoparticles”. All these studies face organic compounds such as strongly polar alkylcyanobiphenyls and mesogenic liquids with different polarities, namely n-heptylcyanobiphenyl and 4-(trans-4'-n-hexylcyclohexyl)isothiocyanatobenzene, whose molecular and prenematic dynamics are investigated [76,96]. Prenematic processes are also studied, through FE evaluation, in organic nonpolar compounds such as admixture of 4-n-ethylcyclohexyl-4'-n-nonylphenyl ( $\text{C}_2\text{H}_5\text{C}_6\text{H}_4\text{P}_h\text{C}_9\text{H}_{19}$ ,  $2\text{C}_y\text{Ph9}$ ) in mesogenic solvent of n-hexylcyanobiphenyl [95], 4-(trans-4'-n-hexylcyclohexyl)isothiocyanatobenzene and 4-cyanophenyl-4'-n-heptylbenzoate [49,50], while in 4-cyanophenyl 4'-alkylbenzoates and 4-n-octyl(4'-cyanophenyl)benzoate the dipolar orientational and isotropy features are correlated to the molecular structures and dielectric properties [48,51].

In Fig. 12 the trend of FE as a function of temperature is displayed for different concentrations of a nonpolar admixture of 4-n-ethylcyclohexyl-4'-n-nonylphenyl in a mesogenic solvent [95]. This is calculated from the dielectric permittivity values reported in Fig. 11 by exploiting the relationship (37) (identical to Eq. (21), which is also recalled in [95]). The trends of dielectric function (Fig. 11) and correlated FE (Fig. 12) are assumed to describe the features of dipole orientation phase transitions, namely the isotropic–nematic (I–N) transition. Hence the critical I–N temperatures are indicated by a sharp increase both of  $\epsilon_s(T)$  and the  $d\epsilon_s/dT$  (dashed line). In other words, the FE plots accurately describe the pretransitional (prenematic) processes. At higher temperatures,  $d\epsilon_s/dT$  is negative: following Fröhlich’s interpretation, this shows a typical disordered polar liquid-like behavior. Lowering temperature a continuous decrease of the disorder is pointed out, also with the change of FE sign, so displaying a further increase of correlation among the molecules. This gradual increasing until the vertical trend of the plots indicates the full I–N transition. It is worth noting that the pure  $2\text{C}_y\text{Ph9}$  without solvent (which is indicated as  $x = 1$  and  $2\text{C}_y\text{Ph9}$  in the plots) shows no FE variation. We here note the specific sensitivity of FE evaluation to pretransitional processes, which is able to describe prenematic behavior in these organic compounds.

#### Organic molecular crystals

Several organic semiconductors raised great interest in research, due to high charge mobilities making them promising materials for

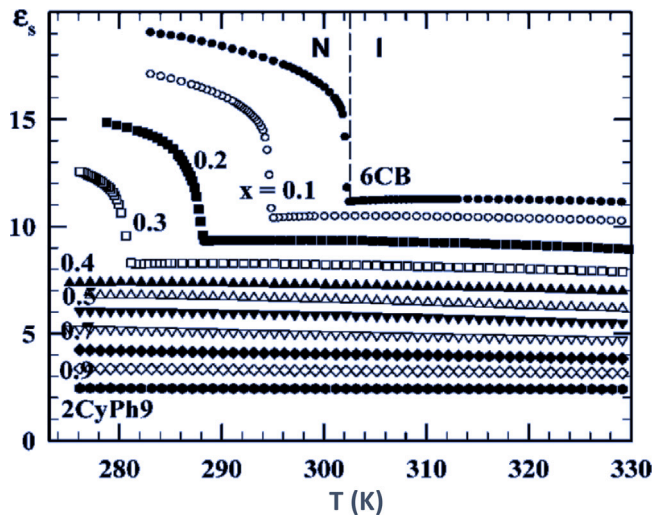


Fig. 11. Dielectric permittivity measured for  $C_6H_{13}PhPhCN$  and  $n$ -hexylcyanobiphenyl mixtures in the isotropic (for the whole concentration range) and the nematic (for  $0 \leq x \leq 0.3$ ) phases as a function of  $T$ . Source: Adapted from [95], Fig. 4.

applications in electronics [97–100]. Among the most studied ones there are rubrene, tetracene, pentacene, and  $\alpha$ -quaterthiophene, which display polymorphism and several different crystalline phases very close in temperature and energy [101–104]. This polymorphic behavior requested a great experimental effort to carefully mapping the material response as a function of temperature and thermodynamic history, for which several techniques were used. In this vein, FE was employed to study the phase evolution and correlated features in molecular crystals. Namely, two pioneering works were carried out on films of  $\alpha$ -quaterthiophene (4T) and tetracene (TEN) crystals [52,53].

Phase transitions

Organic crystalline semiconductors (OCS) typically undergo phase transitions depending on temperature variation [105,106]. Their evolution displays peculiar features: namely, the onset of phase transformations typically are correlated to occurring of instabilities, due to a gradual increase of molecular disorder, causing macroscopic effects.

Such phenomena show analogous features to the pretransitional (or premelting) effects, as e.g. in the previously discussed Ga nanoparticles (Section “Confined metallic nanoparticles”), and can be found in temperature intervals as wide as tens of degrees straddling the specific transition [44]. These pretransitional effects in OCS are usually neglected because they are difficult to be detected. However, taking into account them is mandatory when the critical temperatures and the corresponding instability extension of phases must be identified. Namely, when either low-dimensional or micro- (and nano-) metric samples are considered (thin films, powders, etc.), similarly to what happens in metallic particles, the features of transitions are expected to be correlated to the involved sizes of the considered system. In this vein, FE evaluation can be fruitfully exploited. Specifically, in  $\alpha$ -quaterthiophene (4T) sample, FE behavior is able to provide information about the nature and temperature evolution of the structural transitions. The temperature dependence of the permittivity of single crystal  $\alpha$ -quaterthiophene is shown in Fig. 13 and the corresponding FE in Fig. 14.

In the Plot 13 we see that for the temperature interval between 25 and 190 °C, the  $\epsilon_s$  dielectric function is a nearly constant, with a slight increase in  $T$ . At about 190 °C,  $\epsilon_s$  increases more rapidly with  $T$ , then, at  $T = 201$  °C, it displays a very sharp enhancement. Above 201 °C, the displayed curve further exhibits a positive slope up to  $T_m = 217$  °C and, finally, for  $T > T_m$  the  $\epsilon_s(T)$  curve slope becomes negative. When FE is considered (Fig. 14), a first signal of a transition phenomenon is pointed out by the increasing, starting at 190 °C, of  $S_E$ ; then the subsequent very sharp peak at  $T = 201$  °C represents the critical transition temperature. Above 204 °C, a region where  $S_E$  still remains positive and constant is found. This demonstrates the occurring of a structural transformation between two distinct ordered-solid stable phases with slightly different degrees of order. We observe that this transition starts at 190 °C and it ends at 204 °C, with a temperature extension of about 15 °C. Furthermore, when the temperature arrives to  $T_m = 217$  °C, FE displays a step-like discontinuity without significant pretransitional effects, where entropy changes its sign from positive to negative. Congruently with the discussed Fröhlich’s interpretation, this trend points out a transition from an ordered solid phase ( $FE > 0$ ) to a disordered liquid-like phase ( $FE < 0$ ). Finally, for  $T > T_m$ , FE displays negative constant value, which is the signature of a stable liquid-like system. It is worth noting that the induced  $S_E$  value calculated for 4T in its liquid phase is comparable to the value already found in other organic liquids where FE has been evaluated [47], although it contains different kinds of polar molecules.

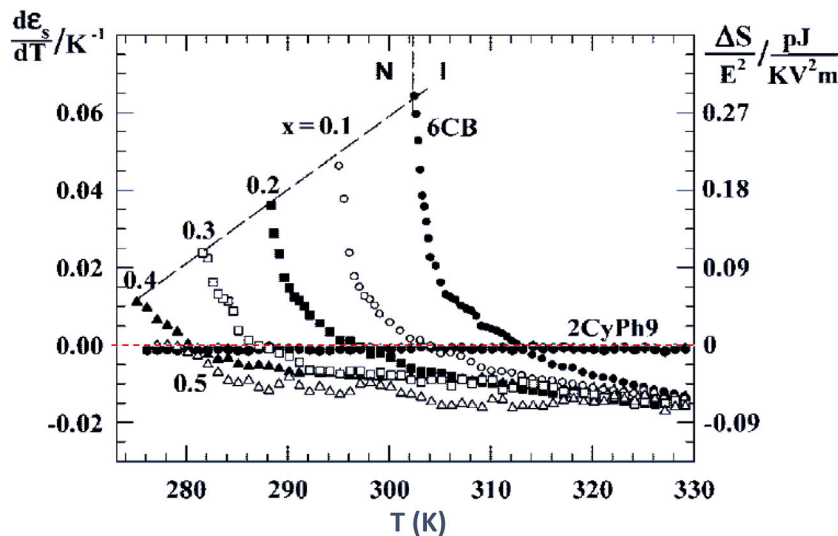


Fig. 12. Critical-like temperature dependence of the dielectric response derivative ( $d\epsilon_s/dT$ ) and the corresponding field-induced increment of the FE (following Eq. (21)) for  $C_6H_{13}PhPhCN$  in  $n$ -hexylcyanobiphenyl mesogenic solutions in the prenematic region. The derivative is calculated from the Plot 11. Source: Adapted from [95], Fig. 6.

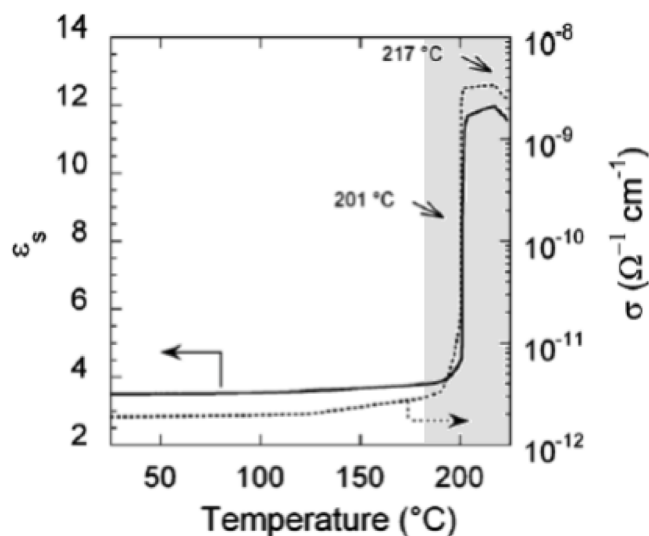


Fig. 13. Measured dielectric response  $\epsilon_s$  and ac conductivity  $\sigma$  (in logarithmic scale) as a function of temperature  $T$  for a 4T sample. Gray color indicates the region where FE is analyzed in Fig. 14 below.

Source: Adapted from [52], Fig. 2a.

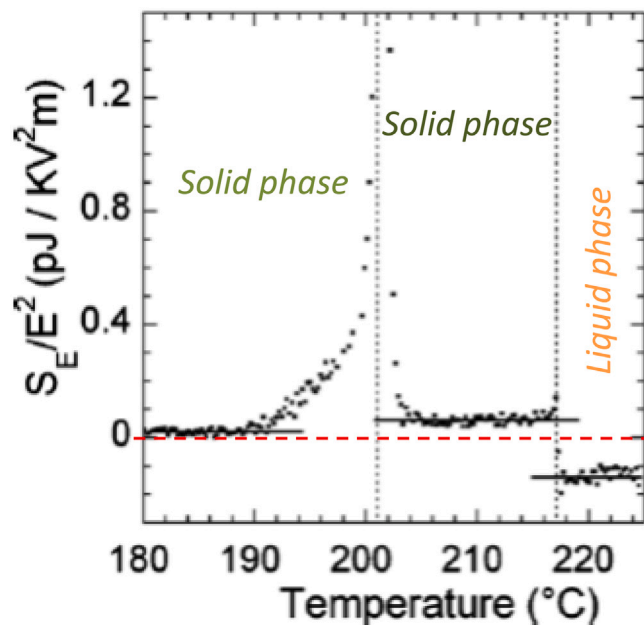


Fig. 14. FE contribution  $S_E/E^2$  as a function of  $T$ , obtained from the derivative of  $\epsilon_s$  in the temperature region 180–225 °C (gray region displayed in Fig. 13) where the solid–solid and solid–liquid transitions occur. The dotted red line highlights the 0-value of FE. The horizontal continuous lines indicate averaged derivative values before and after the two main transitions so highlighting stable phase regions, whose transition critical temperatures are indicated by vertical dotted lines. It is worth noting the first two ordered, solid phases, regions (positive FE) and the last disordered, liquid phase, region (negative FE).

Source: Adapted from [52], Fig. 2b.

Indeed, we conclude that in OCS the FE evaluation technique is able to detect the nature and evolution of temperature-induced phase transition with its extent in temperature and to give a measure of the state-of-order of solid and liquid state.

#### Stability of phases

The issue of evaluating the stability degree of a given phase of matter has been specifically faced on several physical systems. The

usual approach is based on thermodynamic arguments such as Gibbs free energy, entropy, enthalpy and analogous potentials [30,71,73,107–112] which involve several experimental techniques. Congruently, the features of FE evaluation technique make it a good candidate to obtain information about the stability. Actually organic molecular crystals are a paradigmatic class of systems where the stability of phases is an open issue.

A detailed stability analysis was accomplished in TEN crystals [53], where the coexistence of different phases during large temperature intervals had previously been reported [103]. Moreover, this organic compound can be considered a test system because it was investigated by several different experimental techniques, such as X-ray and neutron diffraction, optical and Raman spectroscopies; they showed a complex polymorphism in correlation with thermodynamic parameters [99,103,113–118]. The use of FE estimation on TEN, in comparison with the literature, allowed us to clarify several open issues [53]. Experiments are carried out by accomplishing dielectric measurements in a large temperature region (12–295 K), which are reported in Figs. 15 and 16 for the cooling and heating stages respectively. In Fig. 15a (cooling) three peaks of the permittivity at 50, 153, and 223 K are shown, that point out the occurring of transitions; a strongly perturbed region is found between 125 and 160 K. The corresponding FE plot (Fig. 15b) displays a transition signature at the same temperatures.

Below and immediately above the region of instability, three approximately stable phases, with different levels of order, are evidenced in a near flat FE trend. Above 223 K the continuous increasing with temperature of the FE positive values indicates a progressive marked increase of the correlations between molecules. In the heating stage (Fig. 16) a pronounced different behavior is evidenced. Inspected peaks of permittivity response (Fig. 16a) are much higher and sharper and no perturbed temperature region between peaks is found. FE plot, on the other hand, points out five well-defined signatures of phase transitions, separating six phases (Fig. 16b). The three phases at lowest temperatures (25–45 K, 45–105 K, 105–144 K) display a FE with positive sign and nearly flat trend, indicating a global stability of these phases. On the other hand, the highest temperature phases (144–178 K, 178–207 K and 207–280 K) show strongly changing order state. In particular, the highest temperature phase still displays negative FE values, so indicating a strongly-disordered state. The instability region inspected in cooling stage (Fig. 15b) is explained as an overlapping of the two pointed out phases between 105 K and 178 K [53].

Finally, we also remark that results of Figs. 15 and 16 exhibit a clear non-ergodic response, i.e. a strong dependence on the thermodynamical history of the sample [53,119]. This can be found both in the change of critical temperatures of the inspected transitions and in the change of the state-of-order of the phases.

#### Disordered perovskite crystals

The physical meaningfulness of FE analysis was pinpointed by its application to disordered ferroelectric single crystals, where this experimental approach was also tested to highlight anisotropic features. The analysis is specifically employed to describe the thermal evolution of long-range phases and state-of-order in inorganic perovskites for photonics applications [41,43,54–57,72,120–123], where peculiar dielectric, optical, thermodynamic, and structural effects are still under investigation [55,124–132]. These compounds are known to host<sup>15</sup> nanosized reconfigurable polar regions, the so-called *polar nanoregions* (PNRs), which are mesoscopic regions with inherent electric polarization. These can reconfigure in different states as liquid, solid, and even glassy systems [119,133,137]. Moreover, due to their high dipole moment, they are able to generate giant dielectric susceptibilities ( $\sim 10^4$ – $10^5$ ). This means that the dielectric response of these

<sup>15</sup> below the so-called *Burns temperature* [119,133–136]

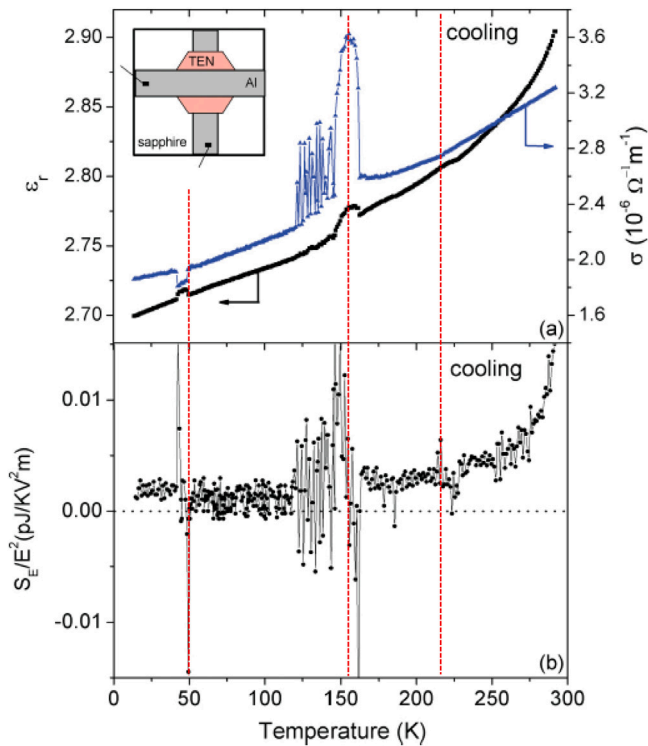


**Fig. 15.** (a) relative dielectric constant  $\epsilon_r$ , and of the conductivity  $\sigma$  vs.  $T$  during cooling stage from RT down to 12 K of a 3- $\mu\text{m}$ -thick TEN single crystal. (b)  $s = s(T)$ , obtained from the derivative of the dielectric constant of Plot (a). We note that the instability in the 125–160 K region is due to the overlapping of two well-distinct transitions, which are highlighted in the heating stroke reported in Plot 16. In both Plots the added vertical dotted red lines indicate the critical temperatures 50, 153, and 223 K. (For interpretation of the references to color in this figure legend, the reader is referred to the web version of this article.)

Source: Adapted from [53], Fig. 1.

materials is essentially due to PNRs and, therefore, that dielectric measurements are the specific technique for investigating their complex and varied evolution, so FE analysis is particularly appropriate [16,54,119,134,135].

### Phase transitions

Compositionally disordered perovskite crystals display a sequence of structural symmetry transformations as a function of temperature [15,17]. Starting from high temperature, the sequence of available configurations<sup>16</sup> is cubic, tetragonal, orthorhombic, rhombohedral. The paradigm of these systems is Barium Titanate ( $\text{BaTiO}_3$ ) [15–17], which displays all these crystalline symmetries. Several works have been devoted to investigate phase transitions in these compounds, e.g. by using NMR and EXAFS techniques [11,12,138]. Namely, as hinted above, PNRs play a key role both in the phase stability and in transition processes. Their structural symmetry, which is different from that of the surroundings, was explored in the tetragonal and orthorhombic phases and they were found to be rhombohedral [7,8]. Nonetheless the features of the PNRs in the low-temperature crystalline phases remain, at present, only partially explored for a very restricted number of compounds (e.g.  $\text{BaTiO}_3$ ,  $\text{SrTiO}_3$ ,  $\text{KNbO}_3$  and  $\text{PbTiO}_3$ ) [119,133–135]. In this vein, the FE evaluation was employed in potassium and tantalum based perovskitic crystals across the cubic-to-tetragonal phase transition [43,55,57]. Actually, works about  $\text{KTa}_{1-x}\text{Nb}_x\text{O}_3$  (KTN) are focused on this transition [43,57,72]. Fig. 17 from [43] points out that when,

<sup>16</sup> depending on the specific kind of perovskite

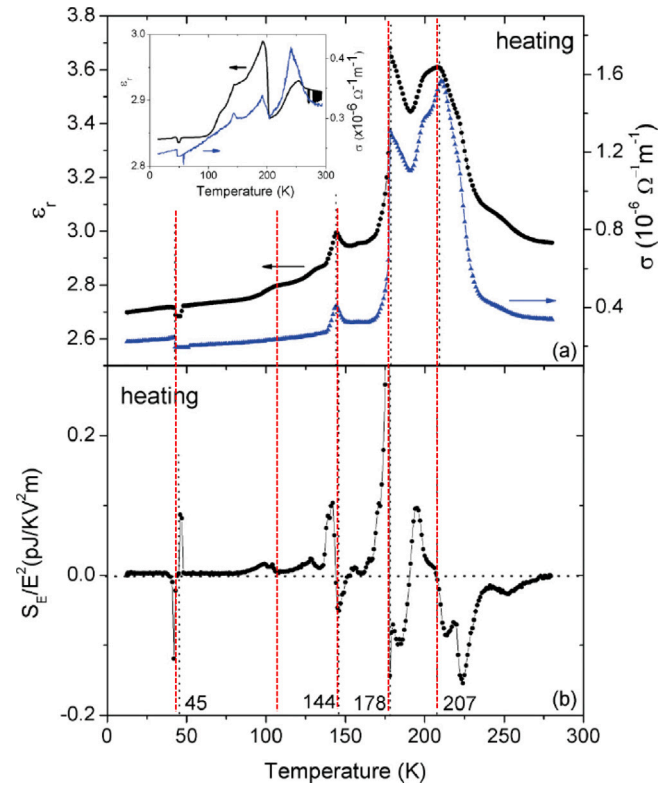


**Fig. 16.** (a) relative dielectric constant  $\epsilon_r$ , and of the conductivity  $\sigma$  vs.  $T$  during heating from 12 K up to RT of the same sample as in Fig. 15 and with the same temperature scan rate. Inset: same as in the main panel (a), but obtained by heating the sample at a higher rate. (b)  $s = s(T)$ , obtained from the derivative of the dielectric constant in Plot (a). In both Plots the added vertical dotted red lines indicate the critical temperatures 45, 105, 144, 178, and 207 K. (For interpretation of the references to color in this figure legend, the reader is referred to the web version of this article.)

Source: Adapted from [53], Fig. 2.

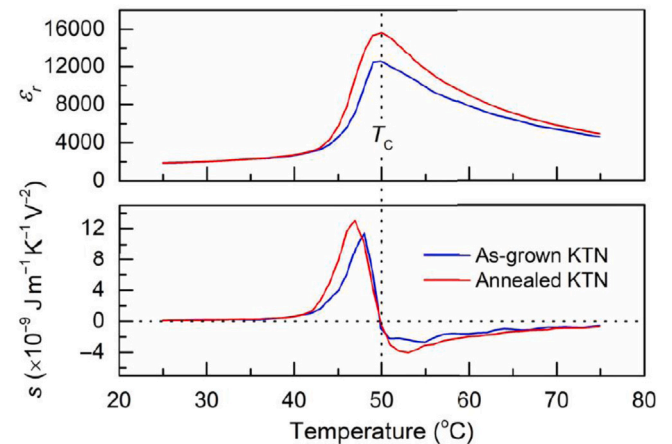


**Fig. 17.** (Top) Dielectric response of KTN and (bottom) correlated FE (following Eq. (21)) across the ferroelectric-to-paraelectric transition. Note that FE plot clearly evidences the critical  $T_c$ .

Source: Adapted from [43], Fig. 4f.

increasing  $T$ , the system passes to a paraelectric state FE evolution signals an order/disorder transition. This demonstrates that a crystalline system following the Curie–Weiss law can be dielectrically considered a liquid of elemental dipoles. These concepts are developed in a much wider temperature region in papers about  $\text{K}_{1-y}\text{Li}_y\text{Ta}_{1-x}\text{Nb}_x\text{O}_3$  (KLTN) [41,55,122] and  $\text{K}_{1-y}\text{Na}_y\text{Ta}_{1-x}\text{Nb}_x\text{O}_3$  [56]. The considered

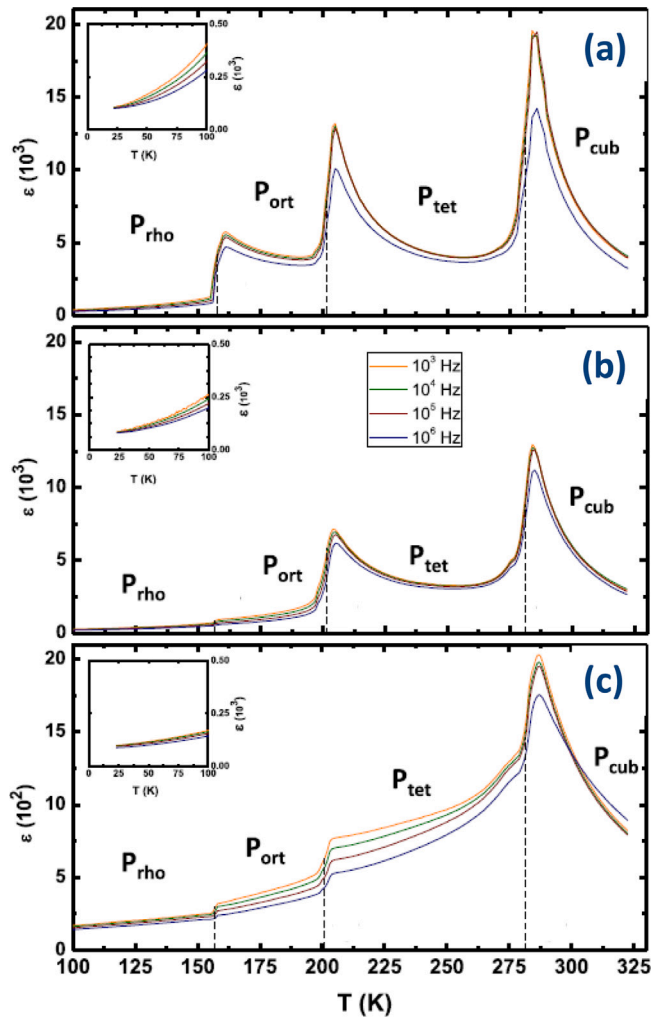


Fig. 18. KLTN relative dielectric permittivity as a function of temperature  $T$  along  $a$  (a),  $b$  (b), and  $c$  (c) perpendicular directions for the cooling stage. The data confirm the prediction by literature for four nominal crystalline phases ( $P_{\text{rho}}$ ,  $P_{\text{ort}}$ ,  $P_{\text{tet}}$ ,  $P_{\text{cub}}$ ). We note a highly anisotropic behavior in all regions.

Source: Adapted from [41], Fig. 2.

samples display four crystalline phases and three transitions along the 320–25 K range, whose dielectric response measurement (Fig. 18 for KLTN) and FE evaluation (Fig. 19 for KLTN and Figs. 20c, 20d for KTN) allows to continuously follow the evolution as a function of temperature. This treatise point out a complex mixture of ordered and disordered phases. We note that FE evaluation enables to identifies all critical temperatures with high precision and points out that transitions are associated to order–disorder changes. More specifically, in KLTN, above each transition, some disordered regions are evidenced (Fig. 19). This phenomenon can be correlated to the arrangement of PNRs, which at high  $T$  region are free-to-reorient, so signaling the presence of a liquid-like system of dipoles. When, in correspondence to the change of FE sign, from negative to positive, the PNRs become correlated and they produce a structured (ordered) configuration. This is indicated by some authors as a glassy state [135,137,139]. Such PNRs configuration continuously evolves and below the FE peak they form large polarized domains giving rise to the ferroelectric arrangement of the tetragonal phase (paraelectric to ferroelectric transition) [140].

Finally, we note that FE oscillations can also be found in such a kind of physical systems (Fig. 2), whose physical meaning is the same as in the previously discussed molecular crystals (Section “Organic molecular crystals”); they point out specific instability regions where, e.g., non-ergodic dynamics can arise (Fig. 15) [53,122].

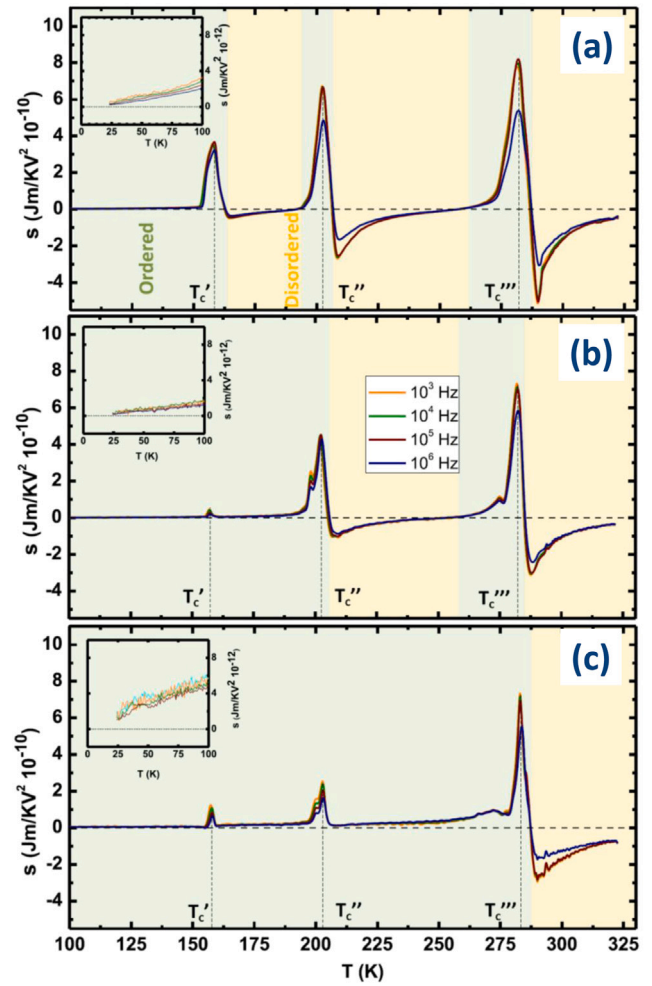


Fig. 19. FE of KLTN (following Eqs. (21) and (25))  $s_a$ ,  $s_b$ ,  $s_c$ , calculated by applying Eq. (21) to the data displayed in Fig. 18, for electric fields applied along, respectively,  $a$  (a),  $b$  (b),  $c$  (c) axes directions (corresponding to [100], [010], and [001] crystalline directions). The indicated temperatures  $T'_c$ ,  $T''_c$ ,  $T'''_c$  for each direction are the identified transition temperatures. The sequence of ordered and disordered regions are highlighted by green and yellow colors respectively. It is worth noting that only the nominally rhombohedral shows stable order features in all directions. (For interpretation of the references to color in this figure legend, the reader is referred to the web version of this article.)

Source: Adapted from [41], Fig. 3.

#### Evolution of the directional order state

The description of the order state evolution depending on  $T$  was proven particularly valid in describing anisotropy. Actually, although the foundation theory is mathematically easy and well established [22, 23,26,29,30], nevertheless it is infrequent to consider thermodynamic quantities as a function of directional physical variables. However, works about disordered perovskites consider FE behavior as a function of crystalline directions, to highlight anisotropic features of their order/disorder state [41,56,57,72]. Actually, these studies exploit the theory of thermodynamic potentials in anisotropic dielectrics which was recently systematically developed [42]. Namely, we can associate the directional FE evaluation therein with Eqs. (23) and (25). The works on KLTN [41], KNTN [56], and KTN [72] point out that these systems undergoes several order/disorder transitions and, in particular, that the feature of either order or disorder depends both on the crystalline phase and the considered direction along which the electric probing field is applied [41,56,72]. Actually, these materials have temperatures where they behave as ordered systems in one direction and disordered



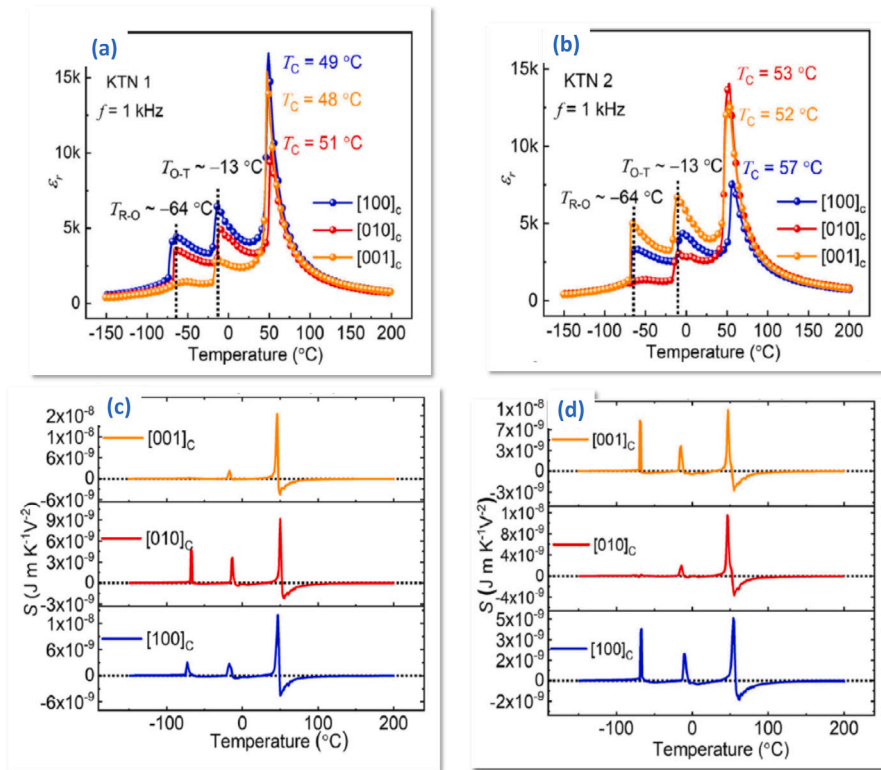


**Fig. 20.** (a) and (b), curves of  $\epsilon'$  versus temperature for two samples of potassium tantalate-niobate (KTN1 and KTN2) which were grown in different strain conditions (see reference). (c) and (d), Fröhlich entropy  $s$  for samples along different directions from KTN1 and KTN2, respectively, the black dotted lines represent  $s = 0$ . Evidence is given of different order state evolution depending on directions.

Source: Adapted from [72], Fig. 2.

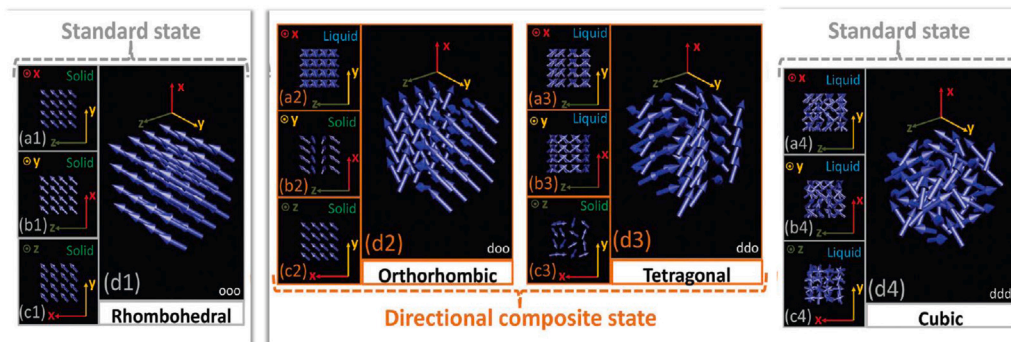


**Fig. 21.** Schematic representation of the dipole arrangement in the four nominal long-range phases of KNTN (it holds for KLTN also). On the opposite ends the two standard states, fully solid and fully liquid respectively. Rhombohedral crystalline phase displaying three solid-like directions (ordered, ordered, ordered, *ooo*): global view (d1) and projections along the axes  $x$ ,  $y$  and  $z$ . Cubic crystalline phase with three liquid-like directions (disordered, disordered, disordered, *ddd*): global view (d4) and projections along the axes  $x$ ,  $y$  and  $z$ . In the middle two exotic liquid–solid directional composite states: orthorhombic crystalline phase with two solid-like and one liquid-like directions (disordered, ordered, ordered, *doo*): global view (d2) and projections along the axes  $x$ ,  $y$  and  $z$ . Tetragonal crystalline phase with one solid-like and two liquid-like directions (disordered, disordered, ordered, *ddo*): global view (d3) and projections along the axes  $x$ ,  $y$  and  $z$ .

Source: Adapted from [56], Fig. 4.

systems in another direction (Fig. 19). This is found in tetragonal and orthorhombic phases, which display unusual arrangement where the system is contemporaneously solid-like in one direction and liquid-like in another. Congruently, these investigations point out that just the highest (nominally cubic) and lowest (nominally rhombohedral) crystalline phases have the same order state in all directions, i.e. disordered and ordered feature respectively (Fig. 19). Being the dielectric response of such systems essentially due to the PNRs, in [56] the authors infer that the correlated FE identify an exotic arrangement of them, whose

schematic depiction is reported in Fig. 21. It is worth observing that directional FE demonstrates that the rhombohedral phase, which is ordered along all directions, is the true stable phase in these relaxors [41,56,72], congruently with what suggested in previous study on similar perovskites [7,8].

We finally stress that both in KLTN and KNTN a remarkable agreement is found between the distribution of the macroscopic order/disorder state as given by FE with the microscopic arrangement of ions as described by the eight-sites model of Comès et al. [1,2,41,56].

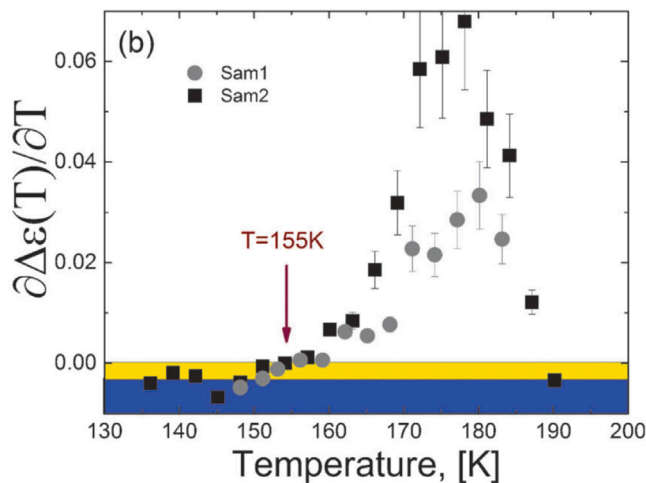


Fig. 22. FE evaluation for two samples (gray circles and black squares, respectively). The parallel tendency of the dipole orientations takes place in the range within the blue background and the short-range orientation is found within the yellow background. (For interpretation of the references to color in this figure legend, the reader is referred to the web version of this article.)

Source: Adapted from [64], Fig. 3.

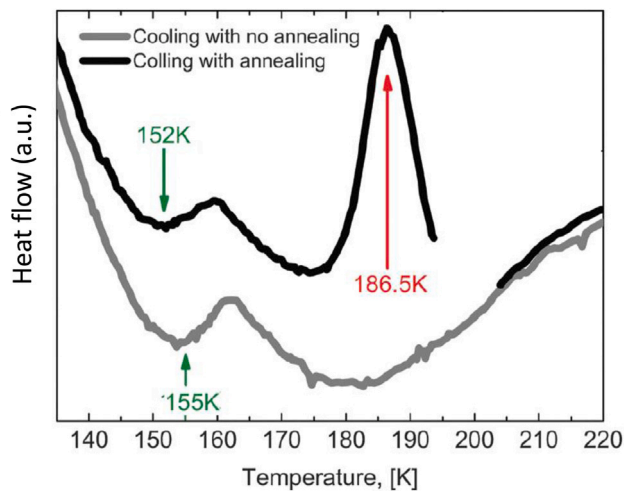


Fig. 23. DSC cooling thermograms of the enzymes sample with (black curve) and without (gray curve) annealing.

Source: Adapted from [64], Fig. 4.

### Other systems

#### Polymeric films

Fröhlich's interpretation was also applied in explaining a dielectric evolution of a polymer-based ferroelectric material, in a work of V.V. Kochervinskii et al. about a copolymer of vinylidene fluoride and tetrafluoroethylene [63]. The paper reports the study on this compound in form of textured films, whose it discusses the molecular mobility and structuring process. In particular, the relationship between the orientational polarization and the topology of structure formation is investigated. The relationship (20) is applied to the dielectric constant at low-frequency. The positive value of  $S_E$  in the investigated temperature region evidences a long-range order in the arrangement of kinetic units participating in the arrangement process of the polymer. These results are in agreement with ferroelectric polymers and with several compounds of this class [141–143].

### Enzymes

A further physical system where FE evaluation has been demonstrated to be able to provide useful information are enzymes, namely globular proteins, which are investigated by Kurzweil-Segev et al. in the framework of complex systems [64]. Actually, the work treats hydrated lysozyme powders with different amount of confined water. Authors carry out a comparison between dielectric and calorimetric measurements in a broad temperature region. The FE data are shown in Fig. 22 and the correlated differential scanning calorimetry (DSC) measurements are depicted in Fig. 23. Comparison of the results from two samples with different water confinement levels is depicted. By correlating dielectric and calorimetric data, the authors remarkably associate the sign change of FE, from negative to positive values, to a glass transition, indicating that complex cooperative processes are acting in hydrated enzymes [64].

### Conclusions

The present review provided the landscape about the exploitation of FE evaluation to inspect the state-of-order in condensed matter. We have highlighted that this approach, which we call *Fröhlich entropy technique*, can be considered a reliable experimental approach for the investigation of several physical systems. Summarizing, the presented method allows the following items:

1. observation of the thermal evolution of the state of order in the sample almost continuously;
2. determination of a stability level of the explored phase;
3. very punctual detection of the phase transitions, critical temperatures with correlated neighborhoods and ordering features;
4. evaluation criterion about the correlation state and consequent rotational freedom of the inherent dipoles;
5. directional investigation highlighting possible anisotropies;
6. relatively easy and not expensive application for the investigation of a wide class of different physical systems in condensed matter.

Congruently we believe that this approach may be fruitfully applied to a set of physical system wider than those here discussed. The presented *Fröhlich entropy estimation technique*, which allows a virtually continuous detection in temperature of the explored sample, on one hand has macroscopic nature, on the other hand gives the possibility to reconstruct information both about macroscopic and mesoscopic phenomena. Then, this technique appears a powerful method complementary to the largely exploited approaches based on local investigation at a fixed temperature.

### Acknowledgment

We thank Prof. E. DelRe for valuable scientific discussions and suggestions.

### References

- [1] Comès R, Lambert M, Guinier A. The chain structure of BaTiO<sub>3</sub> and KNbO<sub>3</sub>. *Solid State Commun* 1968;6:715.
- [2] Comès R, Lambert M, Guinier A. Désordre Linéaire dans les Cristaux (cas du Silicium, du Quartz, et des Pérovskites Ferroélectriques). *Acta Crystallogr Sect A* 1970;26:244.
- [3] Hirota K, Wakimoto S, Cox D. Neutron and X-ray scattering studies of relaxors. *J Phys Soc Japan* 2006;75:111006.
- [4] Buncker G. *Introduction to XAFS*. Cambridge University Press; 2010.
- [5] Faraci G. Nanocluster characterization by EXAFS spectroscopy, in: H.S. Nalwa (Ed.), *Encyclopedia of nanoscience and nanotechnology*.
- [6] Stöhr J. *NEXAFS spectroscopy*. Springer-Verlag; 1991.
- [7] Tsuda K, Sano R, Tanaka M. Nanoscale local structures of rhombohedral symmetry in the orthorhombic and tetragonal phases of BaTiO<sub>3</sub> studied by convergent-beam electron diffraction. *Phys Rev B* 2012;86:214106.

- [8] Tsuda K, Sano R, Tanaka M. Observation of rhombohedral nanostructures in the orthorhombic phase of  $\text{KNbO}_3$  using convergent-beam electron diffraction. *Appl Phys Lett* 2013;102:051913.
- [9] Orauttapong D, Toulouse J, Robertson J, Ye Z. Diffuse neutron scattering study of a disordered complex perovskite  $\text{Pb}(\text{Zn}_{1/3}\text{Nb}_{2/3})\text{O}_3$  crystal. *Phys Rev B* 2001;64:212101.
- [10] Xu G, Shirane G, Copley J, Gehring P. Neutron elastic diffuse scattering study of  $\text{Pb}(\text{Zn}_{1/3}\text{Nb}_{2/3})\text{O}_3$ . *Phys Rev B* 2004;69:064112.
- [11] Zalar B, Laguta V, Blinc R. NMR evidence for the coexistence of order-disorder and displacive components in barium titanate. *Phys Rev Lett* 2003;90:037601.
- [12] Zalar B, Lebar A, Seliger J, Blinc R, Laguta V, Itoh M. NMR study of disorder in  $\text{BaTiO}_3$  and  $\text{SrTiO}_3$ . *Phys Rev B* 2005;71:064107.
- [13] Ishai PB, de Oliveira CEM, Ryabov Y, Feldman Y, Agranat AJ. Glass-forming liquid kinetics manifested in a KTN:Cu crystal. *Phys Rev B* 2004;70:132104.
- [14] Yan X, Liaw P, Zhang Y. Order and disorder in amorphous and high-entropy materials. *Metall Mater Trans A* 2021;52:2111–22.
- [15] Jona F, Shirane G. *Ferroelectric crystals*. New York, USA: Dover; 1993.
- [16] Kao K. *Dielectric phenomena in solids - with emphasis on physical concepts of electronic processes*. San Diego, CA, USA: Elsevier Academic Press; 2004.
- [17] Lines M, Glass A. *Principles and applications of ferroelectrics and related materials*. Oxford, UK: Oxford University Press; 2001.
- [18] Lunkenheimer P, Koehler M, Kastner S, Loidl A. Dielectric spectroscopy of glassy dynamics. In: *Structural glasses and supercooled liquids*. Hoboken, New Jersey, USA: John Wiley & Sons; 2012, p. 115–49. <http://dx.doi.org/10.1002/9781118202470.ch3>.
- [19] Lunkenheimer P, Humann F, Reuter D, Geirhos K, Loidl A, Johari G. Johari-goldstein relaxation in glass electrets. *Phys Rev Mater* 2019;3:112601.
- [20] Coffey WT, Kalmykov YP, editors. *Fractals, diffusion, and relaxation in disordered complex systems: Advances in chemical physics, Part B*. Hoboken, New Jersey, USA: John Wiley & Sons; 2006.
- [21] Rzoska SJ, Zhelezny VP, editors. *Nonlinear dielectric phenomena in complex liquids*. New York, USA: Kluwer Academic Publisher; 2004.
- [22] Devonshire A. Theory of barium titanate - part I. *Phil Mag* 1949;40:1040.
- [23] Scott J. Electrocaloric materials. *Annu Rev Mater Res* 2011;41:229.
- [24] Merz W. Double hysteresis loop of  $\text{BaTiO}_3$  at the curie point. *Phys Rev* 1953;91:513.
- [25] Newhman R. *Properties of materials - Anisotropy, symmetry, structure*. Oxford, UK: Oxford University Press; 2005.
- [26] Nye JF. *Physical properties of crystals - Their representation by tensors and matrices*. Clarendon Press; 1985.
- [27] Ray J. Fluctuations and thermodynamic properties of anisotropic solids. *J Appl Phys* 1982;53:6441–3.
- [28] Narayan O, Young A. Free energies in the presence of electric and magnetic fields. *Amer J Phys* 2005;73:293–8.
- [29] Devonshire A. Theory of ferroelectrics. *Adv Phys* 1954;3:85–130.
- [30] Landau LD, Lifshitz EM. *Electrodynamics of continuous media*. 2nd ed. Oxford, UK: Pergamon Press; 1960.
- [31] Tsao P. Derivation and implications of the symmetry property of the permittivity tensor. *Amer J Phys* 1993;61:823–5.
- [32] Juretschke HJ. Simple derivation of the Maxwell stress tensor and electrostrictive effects in crystals. *Amer J Phys* 1977;45:277–80.
- [33] Johari GP. Effects of electric field on thermodynamics and ordering of a dipolar liquid. *J Chem Phys* 2016;145:164502.
- [34] Fröhlich H. *Theory of dielectrics*. 1st ed. Oxford, UK: Clarendon Press; 1949.
- [35] Fröhlich H. *Theory of dielectrics*. 2nd ed. Oxford, UK: Clarendon Press; 1958.
- [36] Becker R. *Electromagnetic fields and interactions*. Blackie and son; 1964.
- [37] Daniel V. *Dielectric relaxations*. Academic Press; 1967.
- [38] Boettcher CJ. *Theory of electric polarization. Dielectrics in static fields*. Amsterdam, Netherlands: Elsevier; 1973.
- [39] Scaife BKP. *Principles of dielectrics*. 1st ed. Oxford, UK: Clarendon Press; 1989.
- [40] Scaife BKP. *Principles of dielectrics*. 2nd ed. Oxford, UK: Clarendon Press; 1998.
- [41] Parravicini J, DelRe E, Agranat A, Parravicini GB. Macroscopic response and directional disorder dynamics in chemically substituted ferroelectrics. *Phys Rev B* 2016;93:094203.
- [42] Parravicini J. Thermodynamic potentials in anisotropic and nonlinear dielectrics. *Physica B* 2018;541:54–60.
- [43] Tan P, Tian H, Huang F, Meng X, Wang Y, Hu C, Cao X, Li L, Zhou Z. Strain-gradient-controlled disorder dynamics in chemically substituted ferroelectrics. *Phys Rev Appl* 2019;11:024037.
- [44] Parravicini G, Stella A, Tognini P, Merli P, Migliori A, Cheyssac P, Kofman R. Insight into the premelting and melting processes of metal nanoparticles through capacitance measurements. *Appl Phys Lett* 2003;82:1461.
- [45] Parravicini G, Stella A, Ungureanu M, Merli P, Migliori A, Cheyssac P, Kofman R. Phase transitions in gallium nanodroplets detected by dielectric spectroscopy. *Eur Phys J D* 2003;24:219–22.
- [46] Parravicini G, Stella A, Ungureanu M, Merli P, Migliori A, Kofman R. New approach to study melting processes in metal nanoparticles: capacitance measurements. *Phys Status Solidi b* 2003;237:374–80.
- [47] Jadzyn J, Czechowski G. Prenematic behavior of the electric-field-induced increment of the basic thermodynamic quantities of isotropic mesogenic liquids of different polarity. *J Phys Chem B* 2007;111:3727–9.
- [48] Jadzyn J, Sokołowska U, Déjardin J. Temperature behavior of the electric field-induced entropy increment within a homologous series of nematogenic compounds. *J Phys Chem B* 2008;112:9050–2.
- [49] Jadzyn J, Czechowski G, Déjardin J. Dynamics of the self-assembling of mesogenic molecules in the prenematic region of isotropic liquid. *J Phys Chem B* 2008;112:4948–52.
- [50] Jadzyn J, Swiergiel J, Bauman D, Dąbrowski R, Czupryński K, Sokołowska U. Pretransitional dielectric properties of nematogenic 4-cyanophenyl-4'-n-heptylbenzoate. *Phase Transit* 2009;82:409–19.
- [51] Bauman D, Jadzyn J, Wolarz E, Modlińska A, abrowski RD. Dielectric and orientational properties of nematogenic 4-n-octyl(4'-cyanophenyl)benzoate. *Opto-Electron Rev* 2010;18:63–70.
- [52] Sassella A, Braga D, Campione M, Ciabattini T, Moret M, Parravicini J, Parravicini G. Probing phase transitions and stability of organic semiconductor single crystals by dielectric investigation. *J Appl Phys* 2011;109:013529.
- [53] Parravicini G, Campione M, Marabelli F, Moret M, Sassella A. Experimental assessment of nonergodicity in tetracene single crystals. *Phys Rev B* 2012;86:024107.
- [54] Lo Presti L, Parravicini J, Soave R, Parravicini G, Mauri M, Loconte L, Di Mei F, Falsi L, Tartara L, Binetti S, Agranat AJ, DelRe E. Observation of an exotic lattice structure in transparent KTN perovskite and 3D super-crystals. *Phys Rev B* 2020;102:214110.
- [55] DelRe E, Di Mei F, Parravicini J, Parravicini G, Agranat AJ, Conti C. Subwavelength anti-diffracting beams propagating for more than 1,000 Rayleigh lengths. *Nat. Photonics* 2015;9:228.
- [56] Parravicini J, DelRe E, Agranat AJ, Parravicini G. Liquid-solid directional composites and anisotropic dipolar phases of polar nanoregions in disordered perovskite. *Nanoscale* 2017;9:9572.
- [57] Huang F, Hu C, Tian H, Meng X, Tan P, Zhou Z. Controllable anisotropic characteristics in solid solution ferroelectrics. *CrystEngComm* 2019;21:7002–10.
- [58] Matyushov DV. Configurational entropy of polar glass formers and the effect of electrocaloric field on glass transition. *J Chem Phys* 2016;145:034504.
- [59] Johari GP. Effects of electric field on the entropy, viscosity, relaxation time, and glass-formation. *J Chem Phys* 2013;138:154503.
- [60] Johari G. Note: Molecular architecture dependent hydrogen-bonded motifs, entropy change, and dielectric permittivity of alcohols. *J Chem Phys* 2013;139:026101.
- [61] Samanta S, Richert R. Dynamics of glass-forming liquids. XVIII. Does entropy control structural relaxation times? *J Chem Phys* 2015;142:044504.
- [62] Samanta S, Richert R. Electrorheological source of nonlinear dielectric effects in molecular glass-forming liquids. *J Phys Chem B* 2016;120:7737–44.
- [63] Kochervinskii V, Bedin S, Razumovskaya I, Shcherbina M, Buzin M, Malyskhina I, Prazdnichnyi A, Pavlov A, Vasilevskii O. Molecular mobility and structuring in textured films of the ferroelectric copolymer of vinylidene fluoride with tetrafluoroethylene. *Polym Sci A* 2016;58:345.
- [64] Kurzweil-Segev Y, Greenbaum (Gutina) A, Popov I, Golodnitsky D, Feldman Y. The role of the confined water in the dynamic crossover of hydrated lysozyme powders. *Phys Chem Chem Phys* 2016;18:10992–9.
- [65] Vilar J, Rubi J. Communication: System-size scaling of Boltzmann and alternate Gibbs entropies. *J Chem Phys* 2014;140:201101.
- [66] Leuzzi L, Nieuwenhuizen T. *Thermodynamics of the glassy state*. Boca Raton, USA: Taylor and Francis; 2007.
- [67] Dyre JC, Hechsher T, Niss K. A brief critique of the Adam-Gibbs entropy model. *J Non-Crystall Solids* 2009;355:624–7.
- [68] Johari G. Contributions to the entropy of a glass and liquid, and the dielectric relaxation time. *J Chem Phys* 2000;112:7518.
- [69] Johari G. A resolution for the enigma of a liquid's configurational entropy-molecular kinetics relation. *J Chem Phys* 2000;112:8958.
- [70] Sutton C, Levchenko SV. First-principles atomistic thermodynamics and configurational entropy. *Front Chem* 2020;3:757.
- [71] Callen H. *Thermodynamics and an introduction to thermostatistics*. 2nd ed. New York, USA: John Wiley & Sons; 1985.
- [72] Huang F, Hu C, Zhou Z, Meng X, Tan P, Wang Y, Wang C, Tian H. Improving strain in single crystal by composition-gradients design. *Acta Mater* 2020;200:24–34.
- [73] Sethna J. *Statistical mechanics: Entropy, order parameters, and complexity*. 1st ed. Oxford, UK: Oxford University Press; 2006.
- [74] Świergiel J, Jadzyn J. Fractional Stokes-Einstein-Debye relation and orientational entropy effects in strongly hydrogen-bonded liquid amides. *Phys Chem Chem Phys* 2011;13:3911–6.
- [75] Richert R. Nonlinear dielectric effects in liquids: a guided tour. *J Phys Condens Matter* 2017;29:363001.
- [76] Jadzyn J, Déjardin JL, Czechowski G. Singular pretransitional behavior of the electric field-dependent part of the thermodynamic quantities of strongly polar mesogenic liquids in the isotropic phase. *Acta Phys Pol A* 2007;111:877.
- [77] Kaminska E, Tarnacka M, Jurkiewicz K, Kaminski K, Paluch M. High pressure dielectric studies on the structural and orientational glass. *J Chem Phys* 2016;144:054503.
- [78] Nisoli M, Stagera S, De Silvestri S, Stella A, Tognini P, Cheyssac P, Kofman R. Ultrafast electronic dynamics in solid and liquid gallium nanoparticles. *Phys Rev Lett* 1997;78:3575.

- [79] Konrad H, Weissmüller J, Birringer R, Karmonik C, Gleiter H. Phase transitions in gallium nanodroplets detected by dielectric spectroscopy. *Phys Rev B* 1998;58:2142.
- [80] Tognini P, Parravicini G, Stella A, Fornari L, Kofman R, Cheyssac P, Giardini M. Capacitance-conductance investigation on the phase transitions in Ga nanoparticles. *Thin Solid Films* 2000;380:230–2.
- [81] Bernasconi M, Chiarotti GL, Tosatti E. Ab initio calculations of structural and electronic properties of gallium solid-state phases. *Phys Rev B* 1995;52:9988.
- [82] Bosio L, Curien H, Dupont M, Rimsky A. Structure cristalline de Ga $\delta$ . *Acta Crystallogr Sect B* 1973;29:367.
- [83] Parravicini G, Stella A, Ghigna P, Spinolo G, Migliori A, D'Acapito F, Kofman R. Extreme undercooling (down to 90 K) of liquid metal nanoparticles. *Appl Phys Lett* 2006;89:033123.
- [84] Parravicini G, Stella A, Kofman R. New achievements of complex dielectric spectroscopy to study interfaces and nanosystems. *Trends Vacuum Sci Technol* 2004;6:127–39.
- [85] Parravicini G, Stella A, Ungureanu M, Kofman R. Low-frequency negative capacitance effect in systems of metallic nanoparticles embedded in dielectric matrix. *Appl Phys Lett* 2004;85:302.
- [86] Ghigna P, Spinolo G, Parravicini G, Stella A, Migliori A, Kofman R. Metallic versus covalent bonding: Ga nanoparticles as a case study. *J Am Chem Soc* 2007;129:8026–33.
- [87] Jin ZH, Gumbusch P, Lu K, Ma E. Melting mechanisms at the limit of superheating. *Phys Rev Lett* 2001;87:055703.
- [88] Cahn R. Melting from within. *Nature* 2001;413:582.
- [89] Franken J, Marée P, van der Veen JF. Observation of surface-initiated melting. *Phys Rev B* 1986;34:7506.
- [90] Stella A, Cheyssac P, Kofman R, Merli P, Migliori A. Insight into the pre-melting and melting processes of metal nanoparticles through capacitance measurements. *Mater Res Soc Symp Proc* 1996;400:161.
- [91] Jadzyn J, Świergiel J. On similarity of hydrogen-bonded networks in liquid formamide and water as revealed in the static dielectric studies. *Phys Chem Chem Phys* 2012;14:3170–5.
- [92] Płowaś I, Świergiel J, Jadzyn J. Dipolar self-assembling in mixtures of propylene carbonate and dimethyl sulfoxide as revealed by the orientational entropy. *J Phys Chem B* 2016;120:7920–5.
- [93] Świergiel J, Jadzyn J. Temperature behavior of electric relaxational effects due to ionic conductivity in liquid lactones. *Int J Thermophys* 2012;33:783–94.
- [94] Świergiel J, Płowaś I, Grembowski J, Jadzyn J. Stokes-Einstein-Nernst relation in dilute electrolyte solutions of lithium perchlorate in polyethylene glycols (200, 300, 400, and 600). *J Chem Eng Data* 2015;60:3588–93.
- [95] Jadzyn J, Sokołowska U, Czechowski G. The entropy effects in binary mixtures of polar mesogenic solvent/nonpolar solute. *J Phys Chem B* 2008;112:7022–5.
- [96] Jadzyn J, Czechowski G, Déjardin JL. Contribution to understanding of the molecular dynamics in liquids. *J Phys Chem A* 2007;111:8325–9.
- [97] de Boer R, Klapwijk T, Morpurgo A. Field-effect transistors on tetracene single crystals. *Appl Phys Lett* 2003;83:4345.
- [98] Verlaak S, Cheyngs D, Debucquoy M, Arkhipov V, Heremans P. Numerical simulation of tetracene light-emitting transistors: A detailed balance of exciton processes. *Appl Phys Lett* 2004;85:2405.
- [99] Pivovar A, Curtis J, Leao J, Chesterfield R, Frisbie C. Structural and vibrational characterization of the organic semiconductor tetracene as a function of pressure and temperature. *Chem Phys* 2006;325:138.
- [100] Podzorov V, Menard E, Borissav A, Kiryukhin V, Rogers J, Gershenson M. Intrinsic charge transport on the surface of organic semiconductors. *Phys Rev Lett* 2004;93:086602.
- [101] Gundlach D, Jackson T, Schlom D, Nelson S. Solvent-induced phase transition in thermally evaporated pentacene films. *Appl Phys Lett* 1999;74:3302.
- [102] Siegrist T, Kloc C, Schön J, Batlogg B, Haddon R, Berg S, Thomas G. Enhanced physical properties in a pentacene polymorph. *Angew Chem Int Ed Engl* 2001;40:1732.
- [103] Sondermann U, Kutoglu A, Bäessler H. X-ray Diffraction study of the phase transition in crystalline tetracene. *J Phys Chem* 1985;89:1735.
- [104] Della Valle RG, Venuti E, Brillante A, Giraldo A. Inherent structures of crystalline tetracene. *J Phys Chem A* 2006;110:10858.
- [105] Tavazzi S, Campione M. Variable-angle ellipsometry and molecular orientation in monoclinic organic semiconductors. *Appl Phys Lett* 2006;88:071918.
- [106] Campione M, Tavazzi S, Moret M, Porzio W. Crystal-to-crystal phase transition in  $\alpha$ -quaterthiophene: An optical and structural study. *J Appl Phys* 2007;101:083512.
- [107] Landau L, Lifshitz E. *Statistical physics*. 3rd ed. Oxford, UK: Pergamon Press; 1980.
- [108] Kitajgorodskij AI. The principle of close packing and the condition of thermodynamic stability of organic crystals. *Acta Cryst* 1965;18:585.
- [109] Miracle D, Senkov O. A critical review of high entropy alloys and related concepts. *Acta Mater* 2017;122:448–511.
- [110] Muscat J, Swamy V, Harrison N. First-principles calculations of the phase stability of TiO $_2$ . *Phys Rev B* 2002;65:224112.
- [111] Guo S, Liu C. Phase stability in high entropy alloys: Formation of solid-solution phase or amorphous phase. *Proc Natl Sci Mater* 2011;21:433–46.
- [112] Tessier S, Brennecke J, Stadtherr M. Reliable phase stability analysis for excess Gibbs energy models. *Chem Eng Sci* 2000;55:1785–96.
- [113] Prikhotko AF, Skorobogatko AF. *Opt Spectrosc* 1996;20:33.
- [114] Vaubel G, Baessler H. Temperature dependence of width and position of the lowest singlet-singlet transition in crystalline tetracene. *Mol Cryst Liq Cryst* 1970;12:39.
- [115] Kolendrskii DD, Kurik MV, Piriatsinskii YP. Exciton reflection spectra of tetracene single crystals. *Phys Status Solidi b* 1979;91:741.
- [116] Glinski J, Kalinowski J, Stizza S, Bernardini R, Bianconi A. Thermoreflectance spectrum of tetracene single crystal. *Solid State Commun* 1981;38:155.
- [117] Jankowiak R, Kalinowski J, Konys M, Buchert J. Solid-state transitions in crystalline tetracene. *Chem Phys Lett* 1979;56:549.
- [118] Venuti E, Della Valle RG, Farina L, Brillante A, Masino M, Giraldo A. Phonons and structures of tetracene polymorphs at low temperature and high pressure. *Phys Rev B* 2004;70:104106.
- [119] Bokov A, Ye Z. Recent progress in relaxor ferroelectrics with perovskite structure. *J Mater Sci* 2006;41:31–52.
- [120] Parravicini J, Di Mei F, Conti C, Agranat AJ, DelRe E. Diffraction cancellation over multiple wavelengths in photorefractive dipolar glasses. *Opt Express* 2011;19:24109–14.
- [121] Wang Y, Hu C, Tian H, Huang F, Tan P, Wu Y, Wang C, Zhou Z. Electro-optic evolution driven by static and relaxational nano ferroelectric domains in KTa $_{1-x}$ Nb $_x$ O $_3$ . *J Mater Chem C* 2020;8:3235–9.
- [122] Parravicini J, Fornasari L, DelRe E, Marabelli F, Agranat A, Parravicini G. Evidence of double-loop hysteresis in disordered ferroelectric crystal. *J Appl Phys* 2020;127:184107.
- [123] Wang Y, Tan P, Meng X, Zhou Z, Huang X, Hu C, Huang F, Wang J, Tian H. Manganese-doping enhanced local heterogeneity and piezoelectric properties in potassium tantalate niobate single crystals. *IUCr* 2021;8:319–26.
- [124] Parravicini J, Agranat A, Conti C, DelRe E. Rejuvenation in scale-free optics and enhanced diffraction cancellation life-time. *Opt Express* 2012;20:27382.
- [125] Parravicini J, Minzioni P, Degiorgio V, DelRe E. Observation of nonlinear Airy-like beam evolution in lithium niobate. *Opt Lett* 2009;34:3908–10.
- [126] DelRe E, Spinozzi E, Agranat A, Conti C. Scale-free optics and diffractionless waves in nanodisordered ferroelectrics. *Nature Photon* 2011;5:39–42.
- [127] Parravicini J, Agranat A, Conti C, DelRe E. Programming scale-free optics in disordered ferroelectrics. *Opt Lett* 2012;37:2355–7.
- [128] Parravicini J, Pierangeli D, Di Mei F, Conti C, Agranat AJ, DelRe E. Aging solitons in photorefractive dipolar glasses. *Opt Express* 2013;21:30573–9.
- [129] Pierangeli D, Flammini M, Di Mei F, Parravicini J, de Oliveira CEM, Agranat AJ, DelRe E. Continuous solitons in a lattice nonlinearity. *Phys Rev Lett* 2015;114:203901.
- [130] Pierangeli D, Ferraro M, Di Mei F, Di Domenico G, de Oliveira CEM, Agranat A, DelRe E. Super-crystals in composite ferroelectrics. *Nature Commun* 2016;7:10674.
- [131] Di Mei F, Falsi L, Flammini M, Pierangeli D, Di Porto P, Agranat AJ, DelRe E. Giant broadband refraction in the visible in a ferroelectric perovskite. *Nature Photon* 2018;12:734–8.
- [132] Falsi L, Tartara L, Di Mei F, Flammini M, Parravicini J, Pierangeli D, Parravicini G, Xin F, Di Porto P, Agranat AJ, DelRe E. Constraint-free wavelength conversion supported by giant optical refraction in a 3D perovskite super-crystal. *Comms Mater* 2020;1:76.
- [133] Samara GA. The relaxational properties of compositionally disordered ABO $_3$  perovskites. *J Phys: Condens Matter* 2003;15:R367–411.
- [134] Bokov AA, Ye Z-G. Dielectric relaxation in relaxor ferroelectrics. *J Adv Dielect* 2012;2:1241010.
- [135] Toulouse J. The three characteristic temperatures of relaxor dynamics and their meaning. *Ferroelectrics* 2008;369:203–13.
- [136] Burns G, Dacol F. Crystalline ferroelectrics with glassy polarization behavior. *Phys Rev B* 1983;28:2527.
- [137] Pirc R, Kutnjak Z. Electric-field dependent freezing in relaxor ferroelectrics. *Phys Rev B* 2014;89:184110.
- [138] Stern E. Character of order-disorder and displacive components in barium titanate. *Phys Rev Lett* 2004;93:037601.
- [139] Cai L, Toulouse J, Arriger LH, Downing RG, Boatner LA. Origin of the crossover between a freezing and a structural transition at low concentrations in the relaxor ferroelectric K $_{1-x}$ Li $_x$ TaO $_3$ . *Phys Rev B* 2015;91:134106.
- [140] Fu D, Taniguchi H, Itoh M, Mori S. In: Peláiz-Barranco, editor. Pb(Mg $_{1/3}$ Nb $_{2/3}$ )O $_3$  (PMN) Relaxor: Dipole Glass or Nano-Domain Ferroelectric? *IntechOpen*; 2012, p. 51–67. <http://dx.doi.org/10.5772/52139>.
- [141] Kochervinskii V. Low-temperature relaxations and transitions in poly(vinylidene fluoride). *Polym Sci A* 2002;44:20–7.
- [142] Kochervinskii V. The effect of cold drawing of films based on the vinylidene fluoride-tetrafluoroethylene copolymer on molecular mobility in the glass transition region. *Polym Sci A* 2002;44:1137–45.
- [143] Kochervinskii V, Malyskhina I, Markin G, Gavrilova N, Bessonova N. Dielectric relaxation in vinylidene fluoride hexafluoropropylene copolymers. *J Appl Polym Sci* 2007;105:1101.